# Flexible Eu@HOF fabric as highly selective and sensitive optical synapse sensor for six laboratory volatile compounds identification by neuromorphic computing

Xin Xu,[a] and Bing Yan*,[a]

[a] *Shanghai Key Lab of Chemical Assessment and Sustainability, School of Chemical Science and Engineering, Tongji University, Siping Road 1239, Shanghai 200092, China. E-mail: byan@tongji.edu.cn.*

## Electronic supplementary information

## Experimental Section

### Materials and physical measurements

intensity of 362, 484 and 615 nm peaks. (c–d) The concentration-dependent (0–600 ppm) emission spectra of **1-HCl** and emission intensity of 258, 484 and 615 nm peaks.

**Fig. S15.** (a–f) Dependence of emission intensity ratio of 615 and 484 nm peaks on concentration of **Nme**, **Eme**, **Mme**, **Ede**, **TFc** and **HCl**. ($\lambda_{ex}$ = 292 nm).

**Fig. S16.** Response times of **1** toward 600 ppm **Nme** (a), **Eme** (b), **Mme** (c), **Ede** (d), **TFc** (e) and **HCl** (f). ($\lambda_{em}$ = 615 nm).

**Fig. S17.** Emission intensity of 615 nm ($^5D_0 \rightarrow ^7F_2$) emission for **1** after 6, 5, 6, 4, 5 and 5 repetitions with600 ppm **Nme** (a), **Eme** (b), **Mme** (c), **Ede** (d), **TFc** (e) and **HCl** (f) ($\lambda_{ex}$ = 292 nm).

**Fig. S18.** PXRD patterns of **1-Nme**, **1-Eme**, **1-Mme**, **1-Ede**, **1-TFc**, **1-HCl** and **1**.

**Fig. S19.** BPNN diagram indicating the concentration recognition function of **Nme**.

**Fig. S20.** (a) Framework of IsoMe. (b) The single hole of IsoMe with the length (9.2 Å) and width (3.7 Å).

**Fig. S21.** (a–o) 15 LVCs with suitable molecule size that can enter the hole of IsoMe framework. (a) **Nme**, (b) **Eme**, (c) **Mme**, (d) **Ede**, (e) $NH_3$, (f) diethylamine, (g) **HCl**, (h) **TFc**, (i) trifluoromethanesulfonic acid. (j) acetic acid, (k) ethanol, (l) formamide, (m) formaldehyde, (n) chloroform, (o) ethanolamine.

**Fig. S22.** (a–f) 11 LVCs with big molecule size that can't enter the hole of IsoMe framework. (a) trichloroacetic acid, (b) ethyl trifluoacetate, (c) tetrahydrofuran, (d) nitrobenzence, (e) N-hexanol, (f) triethylamine, (g) phenylmethylamine, (h) phenylethylamine, (i) tetramethylammonium hydroxide, (j) benzaldehyde, (k) dodecyl dimethyl tertiary amine.

**Fig. S23.** (a) Emission spectra of Iso and Iso-Ede ($\lambda_{ex}$ = 292 nm). (b) Emission spectra of Me and Me-Ede. (c) The combination of $RNH_2$ (**Nme**, **Eme**, **Mme** and **Ede**) and IsoMe ($\lambda_{ex}$ = 292 nm). (d) The combination of $RNH_2$ (**Nme**, **Eme**, **Mme** and **Ede**) and Iso.

**Fig. S24.** (a–f) EDX mapping of Eu, C, N, O and F elements for **1-TFc**.

**Fig. S25.** EDS spectrum of **1-HCl**, involving the atom contents of Eu, C, N, O and F.

**Fig. S26.** (a–f) EDX mapping of Eu, C, N, O and C; elements for **1-HCl**.

**Fig. S27.** EDS spectrum of **1-TFc**, involving the atom contents of Eu, C, N, O and Cl.

**Fig. S28.** (a) Emission spectra of Me and Me-HCl ($\lambda_{ex}$ = 292 nm). (b) Emission spectra of Iso and Iso-HCl ($\lambda_{ex}$ = 292 nm).

**Fig. S29.** The pictures of the flexible Cu/Ni conductive fabric.

**Fig. S30.** The BPNN 1 training curve.

**Fig. S31.** The BPNN 2 training curve.

**Fig. S32.** (a) Emission and excitation spectra of IsoMe. (b) Phosphorescence lifetime curve of IsoMe by monitoring 488 nm emission peak.

**Table S1.** Summary of phosphorescence decay lifetime of **1**, **1-Eme**, **1-Nme**, **1-Mme**, **1-Ede**, **1-TFc** and **1-HCl**.

**Table S2.** Summary of PL decay lifetime of **1**, **1-Eme**, **1-Nme**, **1-Mme**, **1-Ede**, **1-TFc** and **1-HCl**.

**Table S3.** CIE coordinates of **1** under various excitation from 250 to 400 nm.

**Table S4.** Summary of input and output information during the training of BPNN 1 for classifying six LVCs and blank.

**Table S5.** Network structure information of BPNN 1.

**Table S6.** The summary of mean square error (MSE), original value (OV), calculated value (CV), variance (Var.) for BPNN 1.

**Table S7.** The summary of input and output information in real batch calculation during the test of BPNN 1.

**Table S8.** The matlab code of this BPNN 1.

**Table S9.** Summary of fluorescence sensing parameters of **1** for detecting **Nme**, **Eme**, **Mme**, **Ede**, **TFc** and **HCl**.

**Table S10.** Summary of input and output information during the training of BPNN 2 for recognizing the concentration of **Nme**.
**Table S11.** Network structure information of BPNN 2.
**Table S12.** The summary of mean square error (MSE), original value (OV), calculated value (CV), variance (Var.) of BPNN 2.
**Table S13.** The summary of input and output information in real batch calculation during the test of BPNN 2.
**Table S14.** The matlab code of this BPNN 2.

## Experimental Section

### Materials and physical measurements

$Eu(NO_3)_3{\cdot}6H_2O$ was prepared by dissolving $Eu_2O_3$ (99.99%) solids in 68% nitric acid with recrystallization. All quinolones (≥98%) such as N-propylamine, ethylamine, methylamine, ethylenediamine, trifluoroacetic acid, hydrochloric acid, ammonia, phenylethylamine, diethylamine, triethylamine, phenylmethylamine, ethanolamine, dodecyl dimethyl tertiary amine, trichloroacetic acid, acetic acid, hydrochloric acid, methanol, chloroform, formamide, trifluorometha nesulfonic acid, N-hexanol, tetrahydrofuran, formaldehyde, tetramethylammonium hydroxide, nitrobenzence, ethyl trifluoacetate and benzaldehyde were all purchased from Sigma-Aldrich. Other regents were used without further purification. Powder X-ray diffraction (PXRD) patterns were collected with a Bruker D8 ADVANCE diffractometer using Cu *Kα* radiation at 40 mA and 40 kV. SEM was performed on a Hitachi S-4800 field emission scanning electron microscope operating at 3 kV. Energy dispersive X-ray spectroscopy (EDX) and the EDX mapping image were obtained by the scanning electron microscope operating at 15 kV. X-ray photoelectron (XPS) spectra were recorded under ultrahigh vacuum (<10−6 Pa) at a pass energy of 93.90 eV with an Axis Ultra DLD spectrometer (Kratos) by using a Mg K*α* (1253.6 eV) anode. All binding energies were adjusted by using contaminant carbon (C 1s = 284.8 eV). Fourier transform infrared (FT-IR) spectra were recorded using a Nicolet IS10 infrared spectrophotometer. The photoluminescence (PL) spectra, kinetics scan curve and phosphorescence decay lifetime curve were recorded on an Edinburgh FLS920 spectrophotometer with a 450 W xenon lamp as an excitation source. Photoluminescence lifetime measurements were measured on the Edinburgh FLS920 spectrophotometer with a microsecond lamp (100 mW)

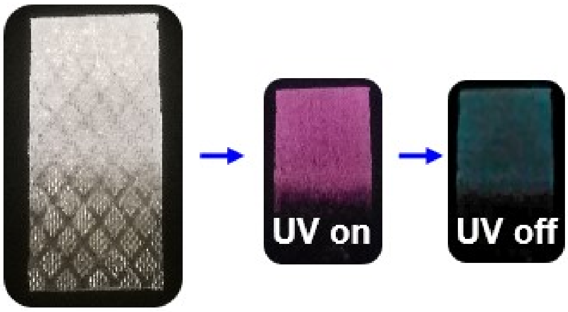


**Fig. S1.** Picture of **1** under daylight, 290 nm UV light (on) and 290 nm UV light (off).

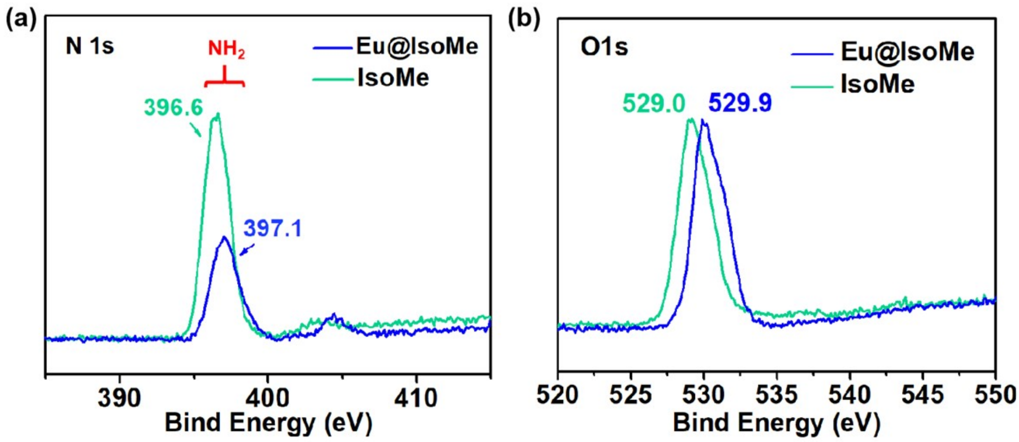


**Fig. S2.** (a) XPS spectra of N 1s electron in Eu@IsoMe and IsoMe. (b) XPS spectra of O 1s electron in Eu@IsoMe and IsoMe.

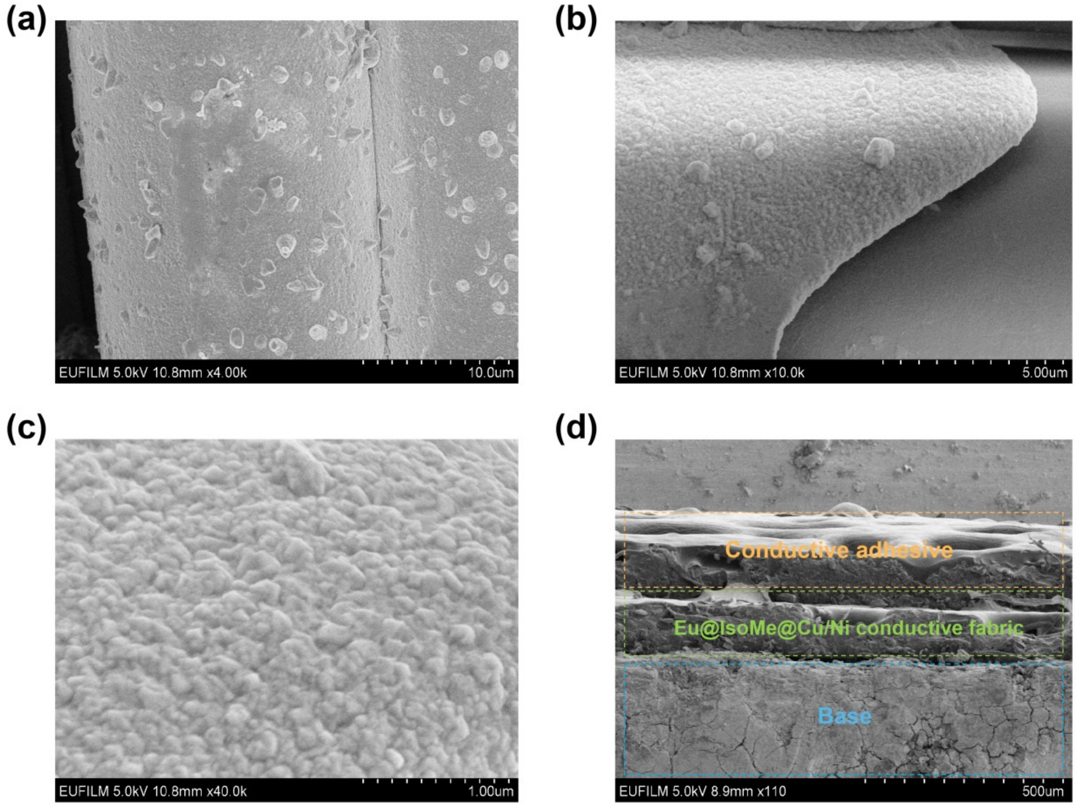


**Fig. S3.** (a−d) SEM diagrams of **1** in various resolutions of 10, 5, 1 and 500 μm.

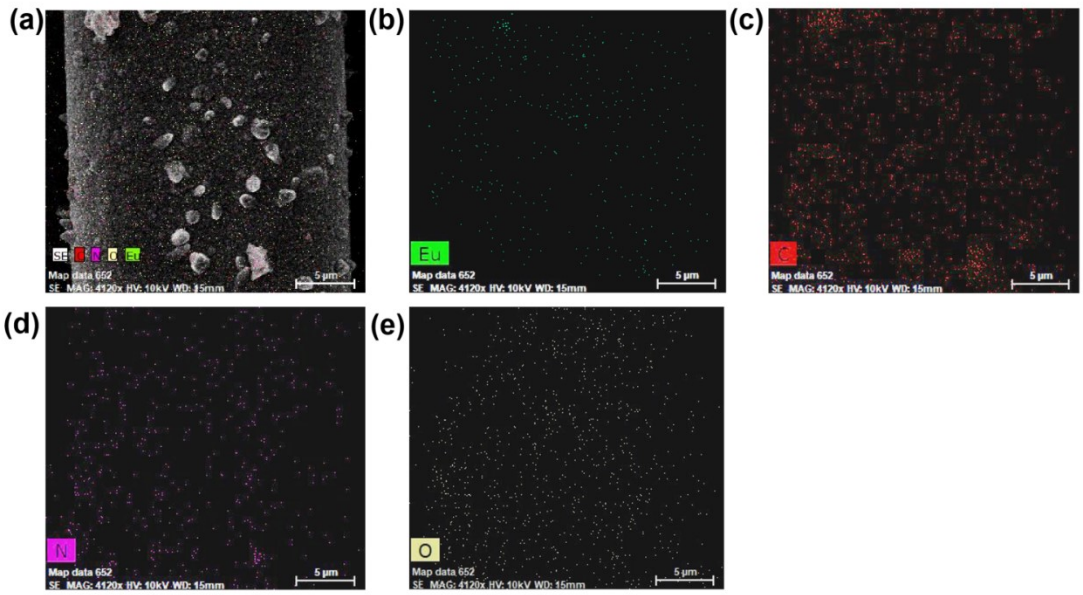


**Fig. S4.** (a−e) EDX mapping of Eu, C, N, and O elements for **1**.

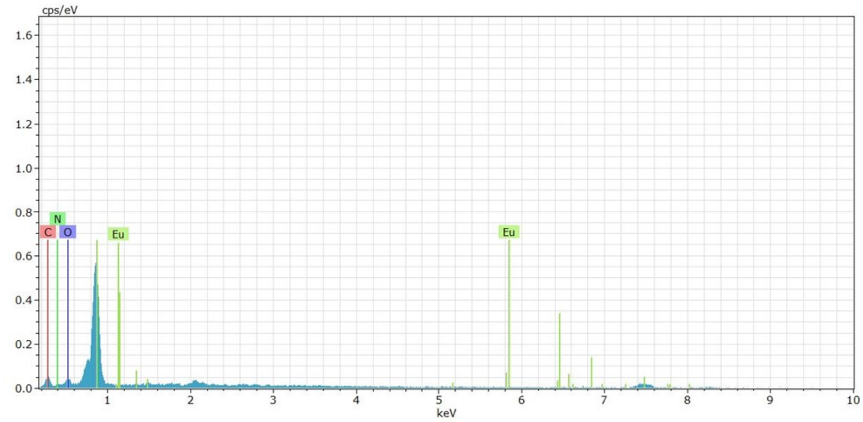


**Fig. S5.** EDS spectrum of **1**, involving the atom contents of Eu (7.97%), C (47.86%), N (13.73%) and O (30.44%).

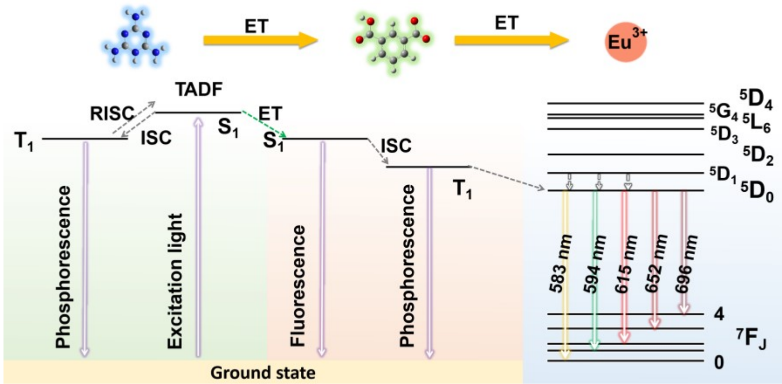


**Fig. S6.** Schematic diagram for photoluminescence mechanism of Eu@IsoMe. (ISC: intersystem crossing; RISC: reverse intersystem crossing; TADF: thermally activated delayed fluorescence)

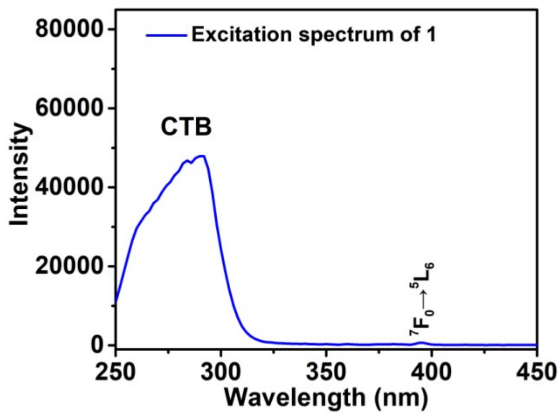


**Fig. S7.** Excitation spectrum of **1** ($\lambda_{em}$ = 615 nm).

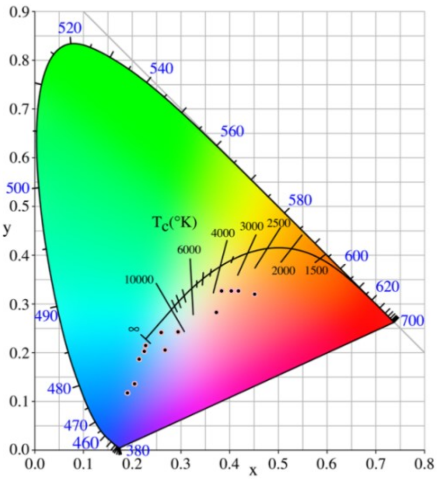

**Fig. S8.** CIE diagram of **1** for its 3D EEM ($\lambda_{ex}$ = 250−400 nm).

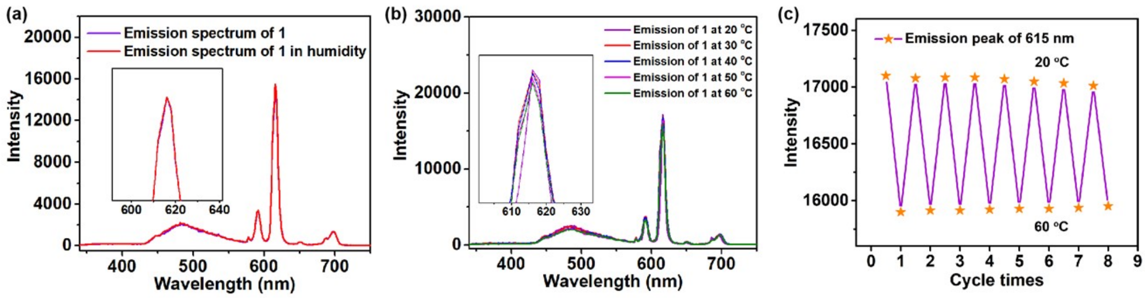


**Fig. S9.** (a) Emission spectra of **1** and **1** in humidity ($\lambda_{ex}$ = 292 nm). (b) Emission spectra of **1** at 20, 30, 40, 50 and 60 °C ($\lambda_{ex}$ = 292 nm). (c) The cycle experiment of **1** in temperature range of 20−60 °C.

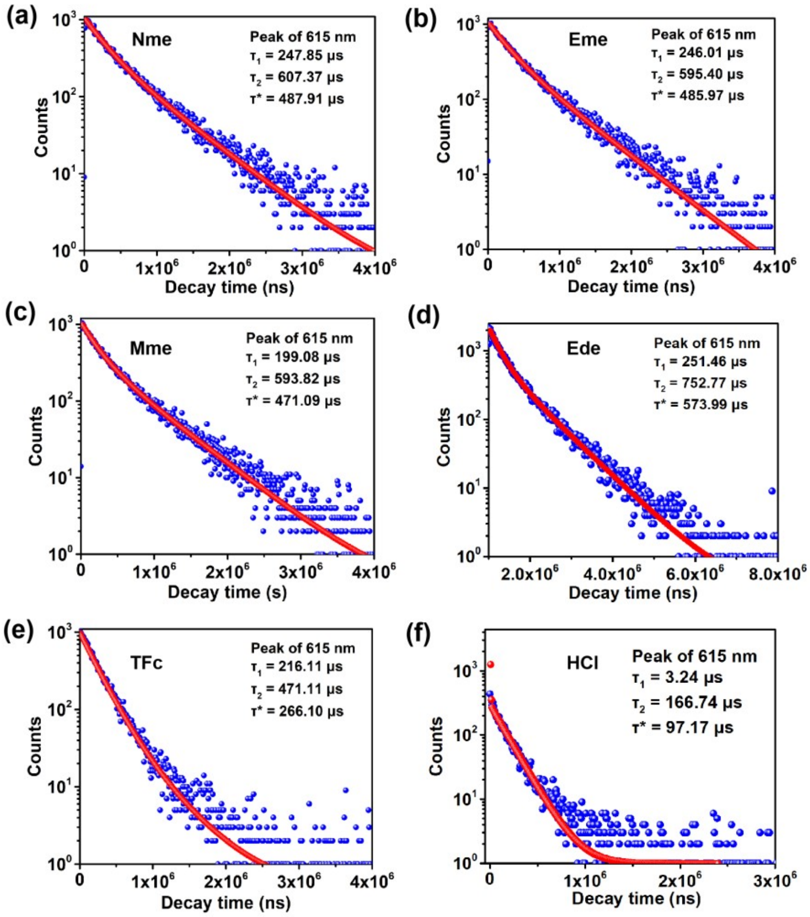


**Fig. S10.** PL lifetimes of 615 nm emission peak for **1-Nme** (a), **1-Eme** (b), **1-Mme** (c), **1-Ede** (d), **1-TFc** (e), **1-HCl** (f).

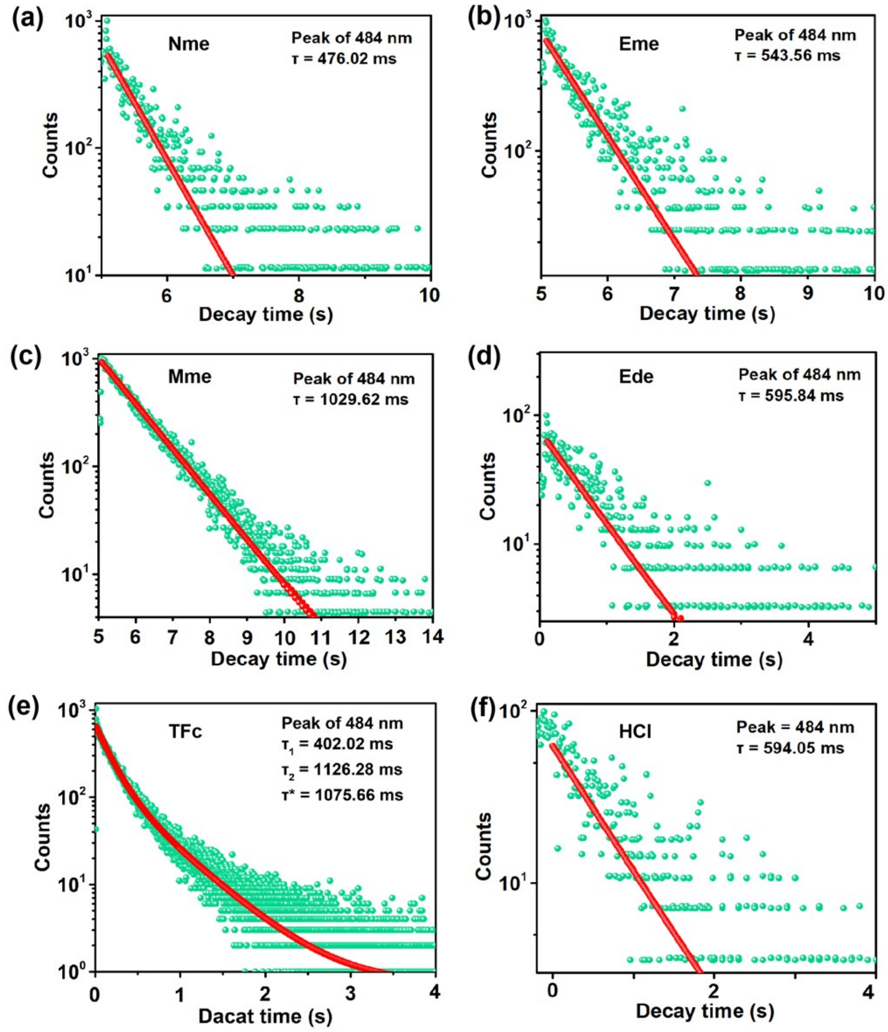


**Fig. S11.** Phosphorescence lifetimes of 484 nm emission peak for **1-Nme** (a), **1-Eme** (b), **1-Mme** (c), **1-Ede** (d), **1-TFc** (e), **1-HCl** (f).

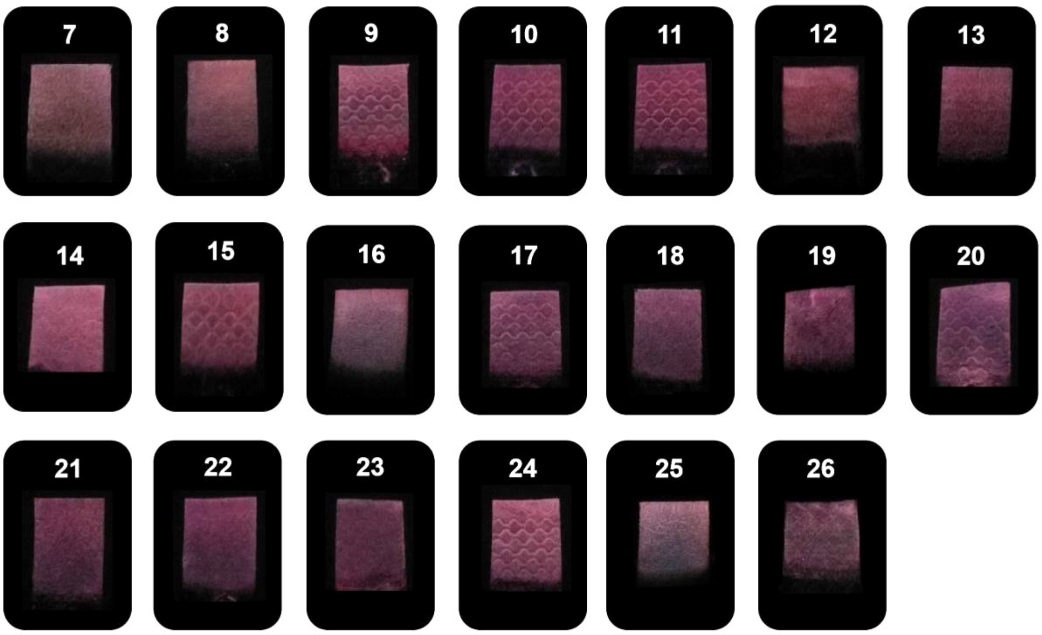


**Fig. S12.** Emitting pictures of **1** in various LVC atmospheres under 290 nm UV light, which involving ammonia (5), phenylethylamine (6), diethylamine (7), triethylamine (8), phenylmethylamine (9), ethanolamine (10), dodecyl dimethyl tertiary amine (11), trichloroacetic acid (13), acetic acid (14), methanol (16), chloroform (17), trifluorometha nesulfonic acid (18), N-hexanol (19), tetrahydrofuran (20), formaldehyde (21), formamide (22), tetramethylammonium hydroxide (23), nitrobenzence (24), ethyl trifluoacetate (25) and benzaldehyde (26). (600 ppm, UV lamp: 8 W)

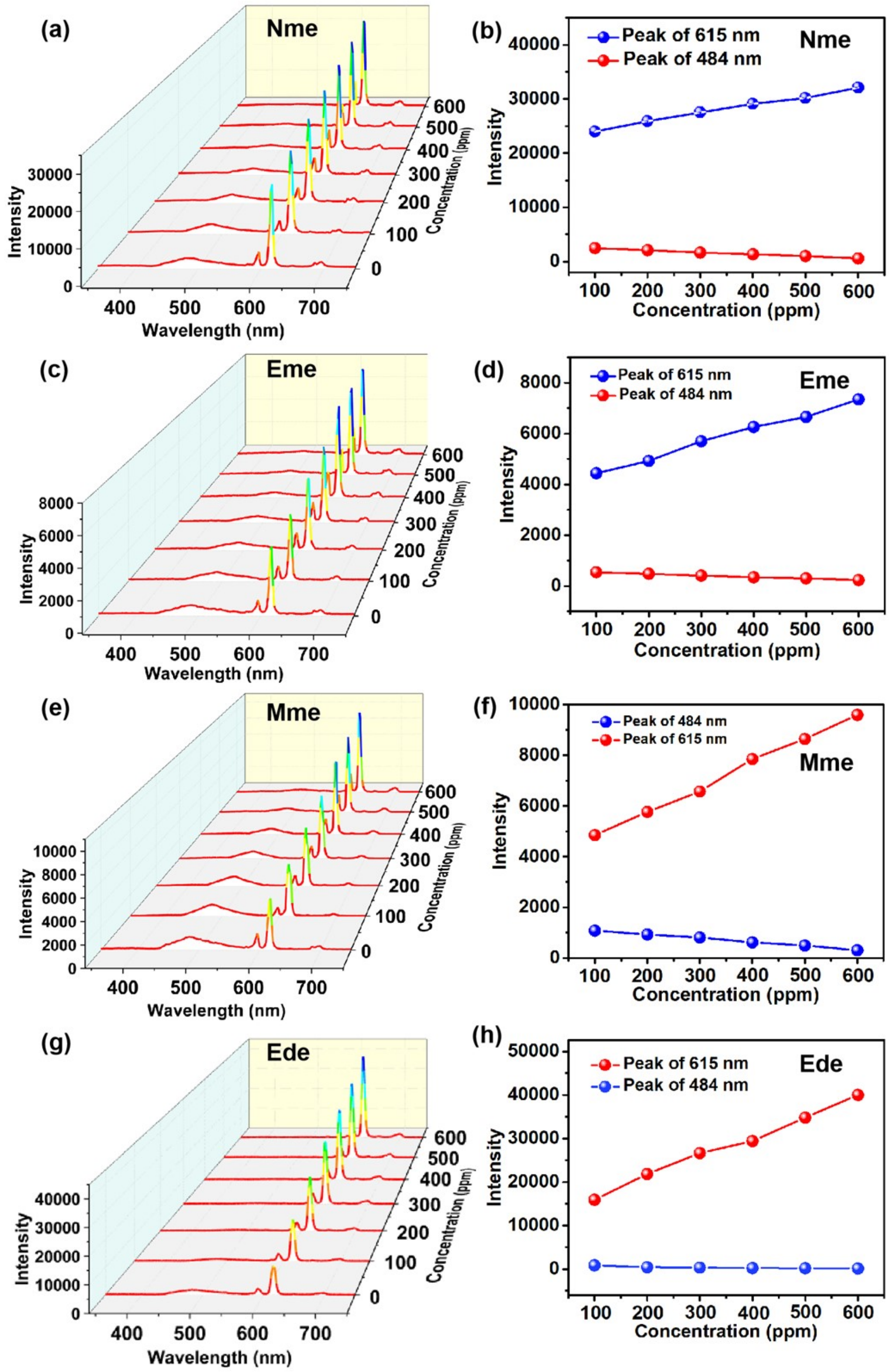


**Fig. S13.** (a−b) The concentration-dependent (0−600 ppm) emission spectra of **1-Nme** and emission intensity of 484 and 615 nm peaks. (c−d) The concentration-dependent (0−600 ppm) emission spectra of **1-Eme** and emission intensity of 484 and 615 nm peaks. (e−f) The concentration-dependent (0−600 ppm) emission spectra of **1-Mme** and emission intensity of 484 and 615 nm peaks. (g−h) The concentration-dependent (0−600 ppm) emission spectra of **1-Ede** and emission intensity of 484 and 615 nm peaks.

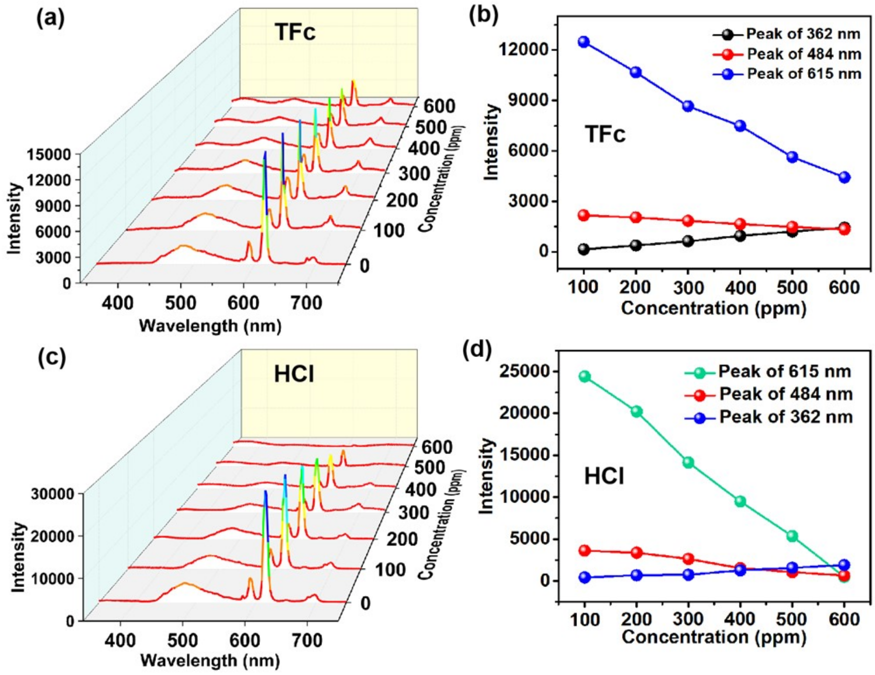


**Fig. S14.** (a−b) The concentration-dependent (0−600 ppm) emission spectra of **1-TFc** and emission intensity of 362, 484 and 615 nm peaks. (c−d) The concentration-dependent (0−600 ppm) emission spectra of **1-HCl** and emission intensity of 258, 484 and 615 nm peaks.

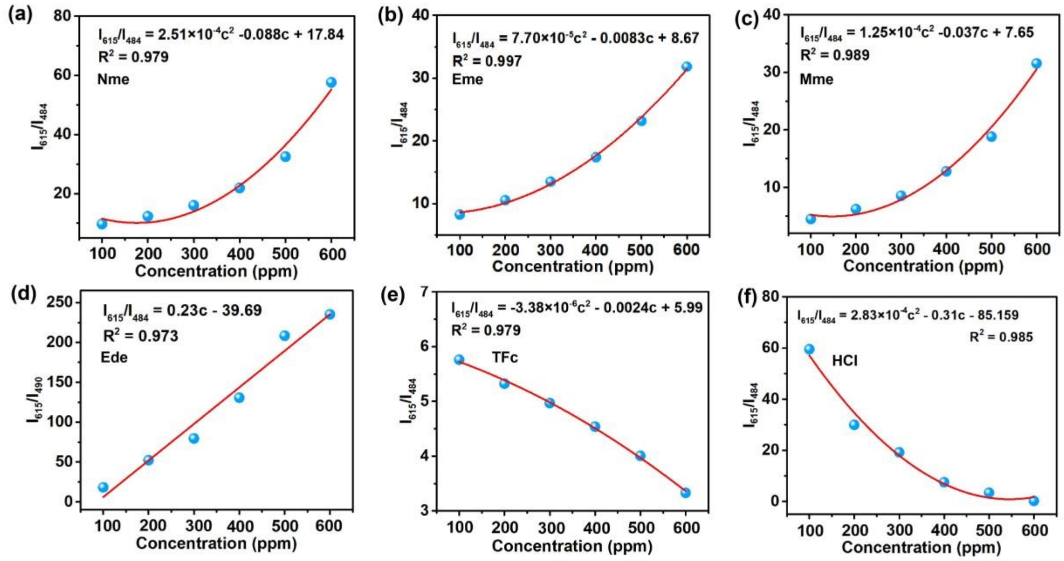


**Fig. S15.** (a−f) Dependence of emission intensity ratio of 615 and 484 nm peaks on concentration of **Nme**, **Eme**, **Mme**, **Ede**, **TFc** and **HCl**. ($\lambda_{ex}$ = 292 nm).

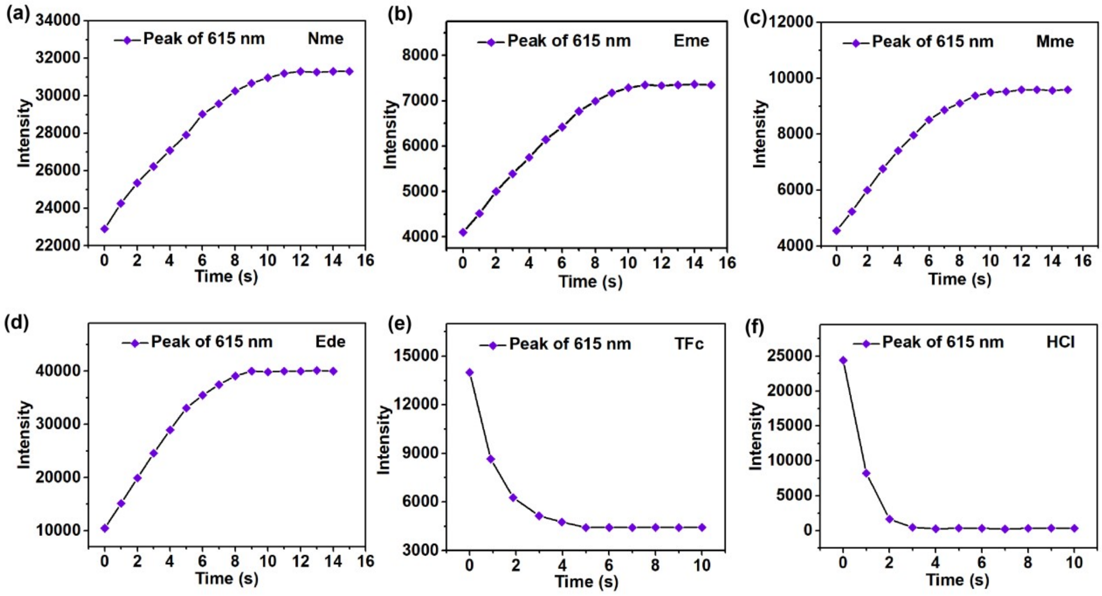


**Fig. S16.** Response times of **1** toward 600 ppm **Nme** (a), **Eme** (b), **Mme** (c), **Ede** (d), **TFc** (e) and **HCl** (f). ($\lambda_{em}$ = 615 nm).

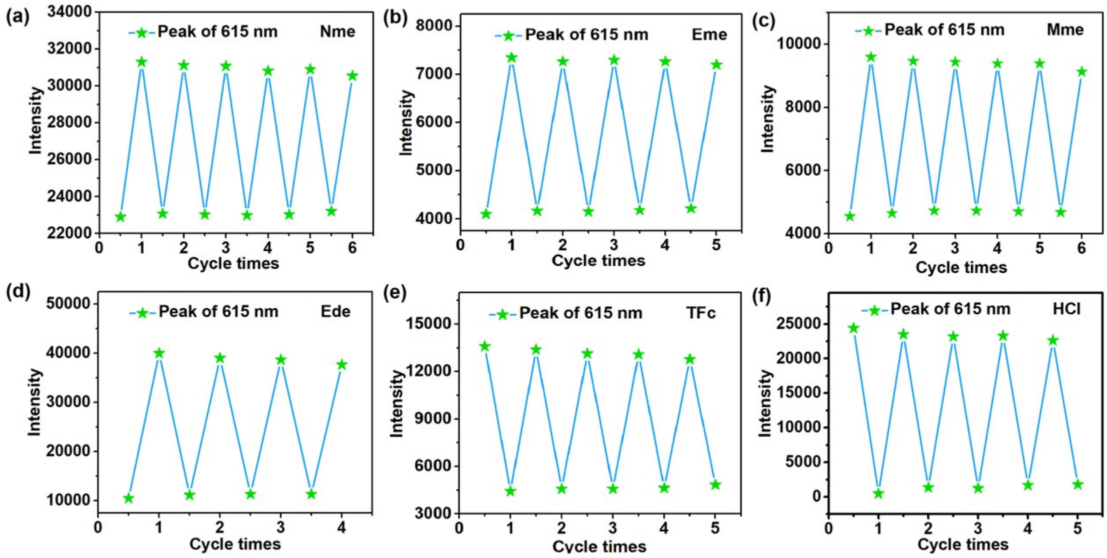


**Fig. S17.** Emission intensity of 615 nm ($^5D_0 \rightarrow ^7F_2$) emission for **1** after 6, 5, 6, 4, 5 and 5 repetitions with 600 ppm **Nme** (a), **Eme** (b), **Mme** (c), **Ede** (d), **TFc** (e) and **HCl** (f) ($\lambda_{ex}$ = 292 nm).

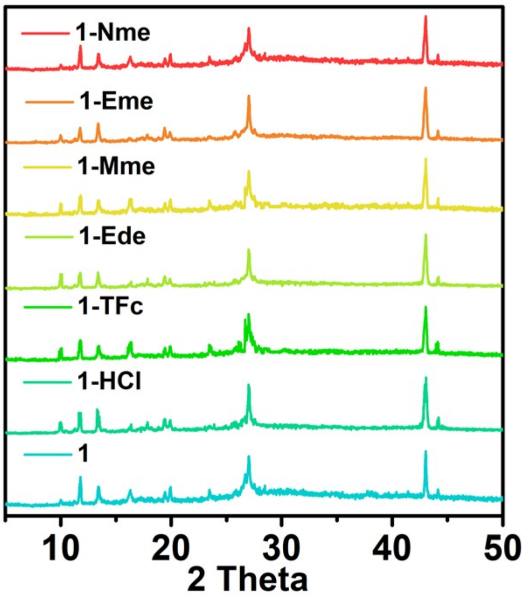


**Fig. S18.** PXRD patterns of **1-Nme**, **1-Eme**, **1-Mme**, **1-Ede**, **1-TFc**, **1-HCl** and **1**.

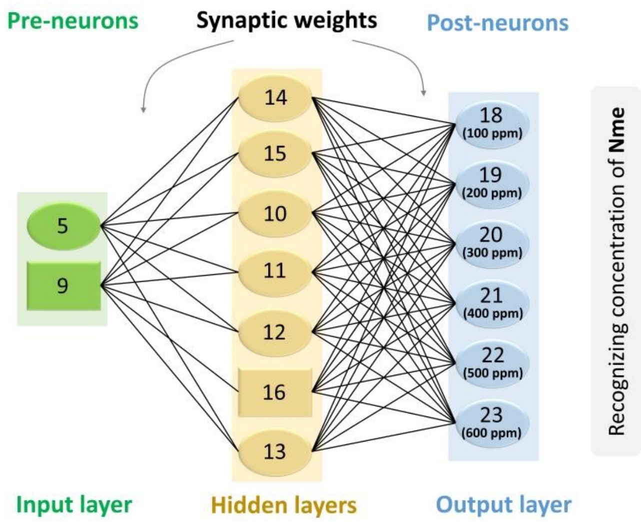


**Fig. S19.** BPNN diagram indicating the concentration recognition function of **Nme**.

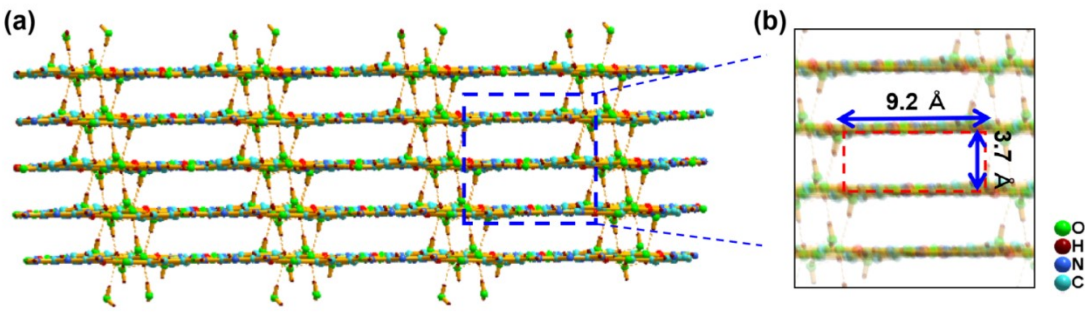


**Fig. S20.** (a) Framework of IsoMe. (b) The single hole of IsoMe with the length (9.2 Å) and width (3.7 Å).

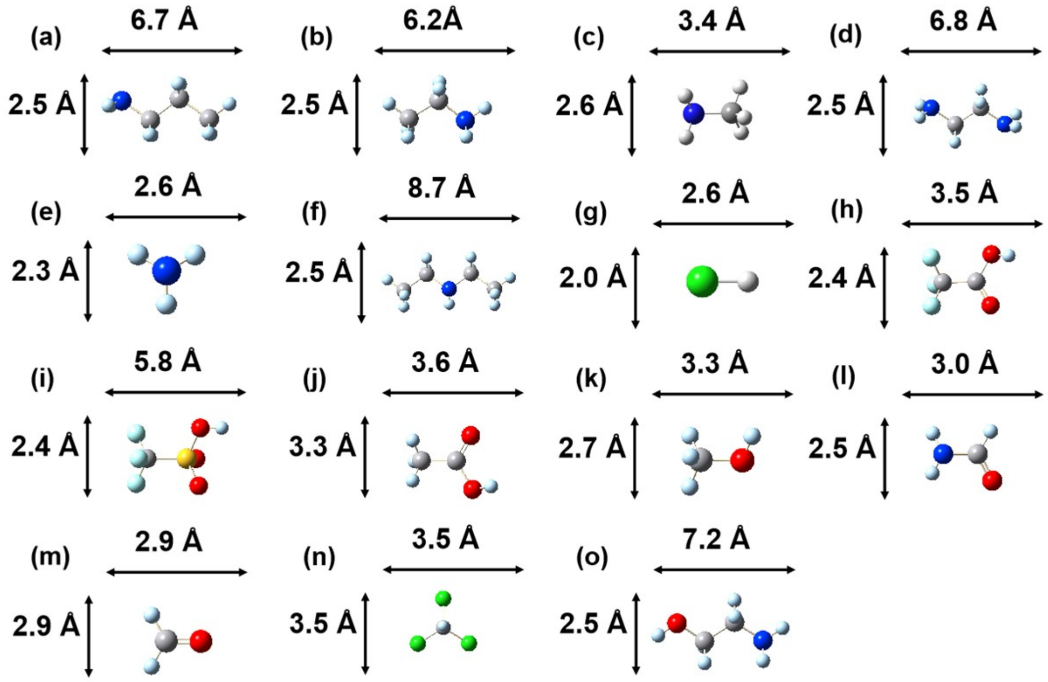


**Fig. S21.** (a−o) 15 LVCs with suitable molecule size that can enter the hole of IsoMe framework. (a) **Nme**, (b) **Eme**, (c) **Mme**, (d) **Ede**, (e) $NH_3$, (f) diethylamine, (g) **HCl**, (h) **TFc**, (i) trifluoromethanesulfonic acid. (j) acetic acid, (k) ethanol, (l) formamide, (m) formaldehyde, (n) chloroform, (o) ethanolamine.

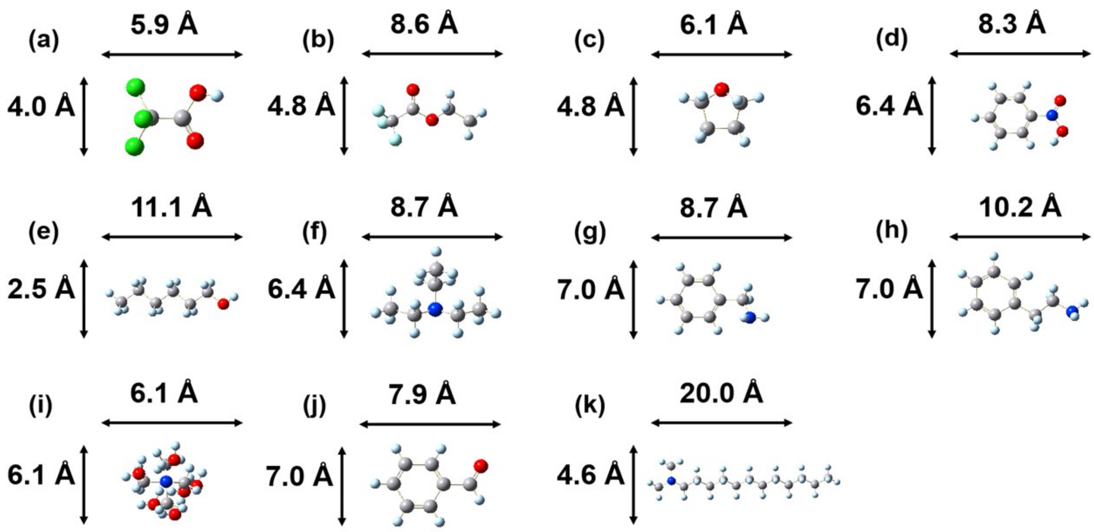


**Fig. S22.** (a−f) 11 LVCs with big molecule size that can't enter the hole of IsoMe framework. (a) trichloroacetic acid, (b) ethyl trifluoacetate, (c) tetrahydrofuran, (d) nitrobenzence, (e) N-hexanol, (f) triethylamine, (g) phenylmethylamine, (h) phenylethylamine, (i) tetramethylammonium hydroxide, (j) benzaldehyde, (k) dodecyl dimethyl tertiary amine.

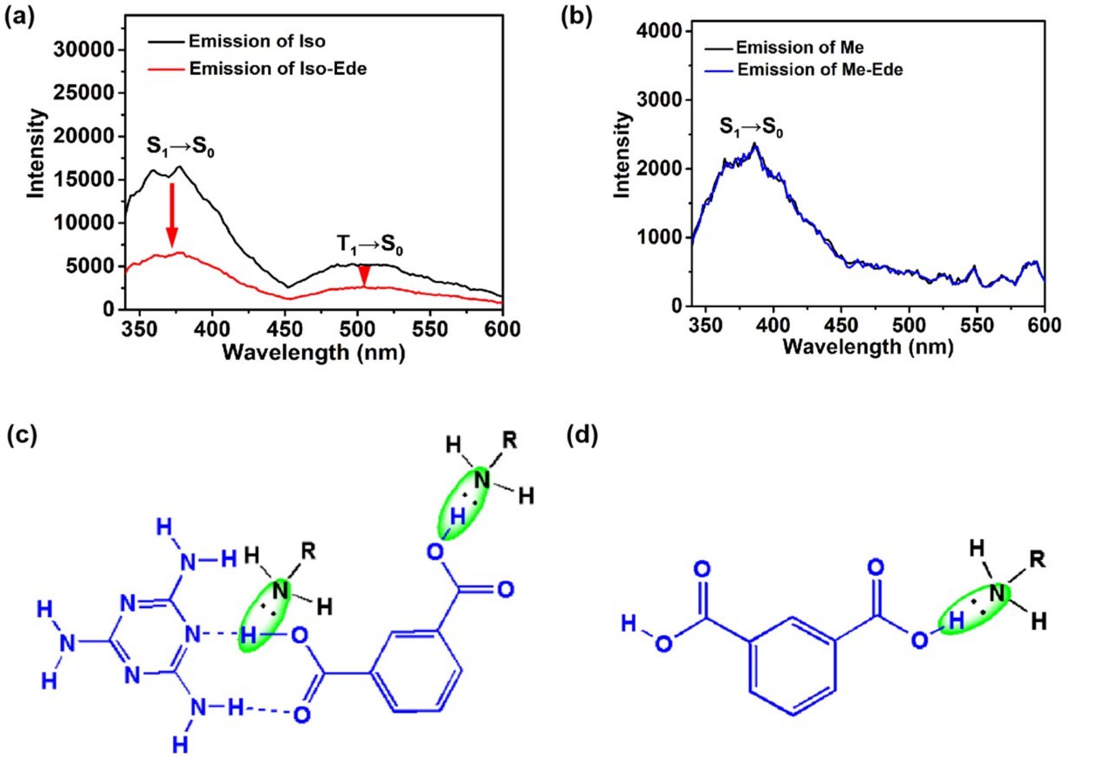


**Fig. S23.** (a) Emission spectra of Iso and Iso-Ede ($\lambda_{ex}$ = 292 nm). (b) Emission spectra of Me and Me-Ede. (c) The combination of $RNH_2$ (**Nme**, **Eme**, **Mme** and **Ede**) and IsoMe ($\lambda_{ex}$ = 292 nm). (d) The combination of $RNH_2$ (**Nme**, **Eme**, **Mme** and **Ede**) and Iso.

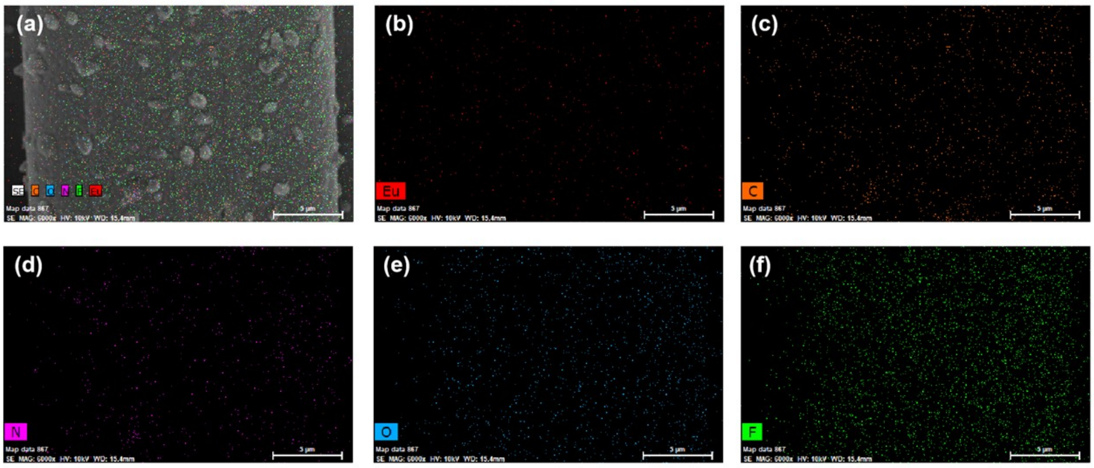


**Fig. S24.** (a−f) EDX mapping of Eu, C, N, O and F elements for **1-TFc**.

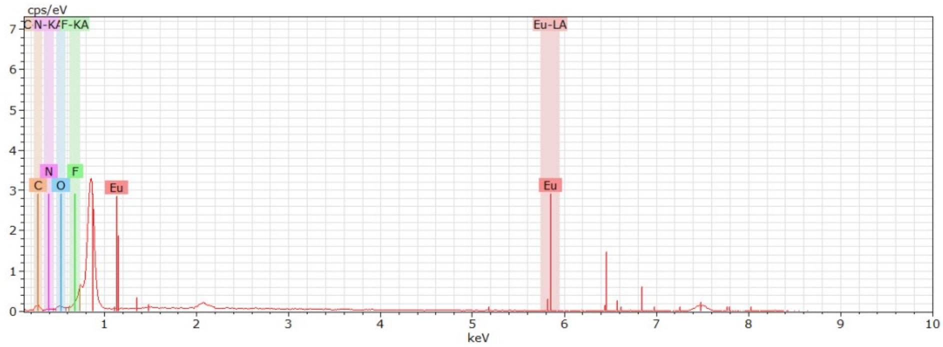


**Fig. S25.** EDS spectrum of **1-HCl**, involving the atom contents of Eu, C, N, O and F.

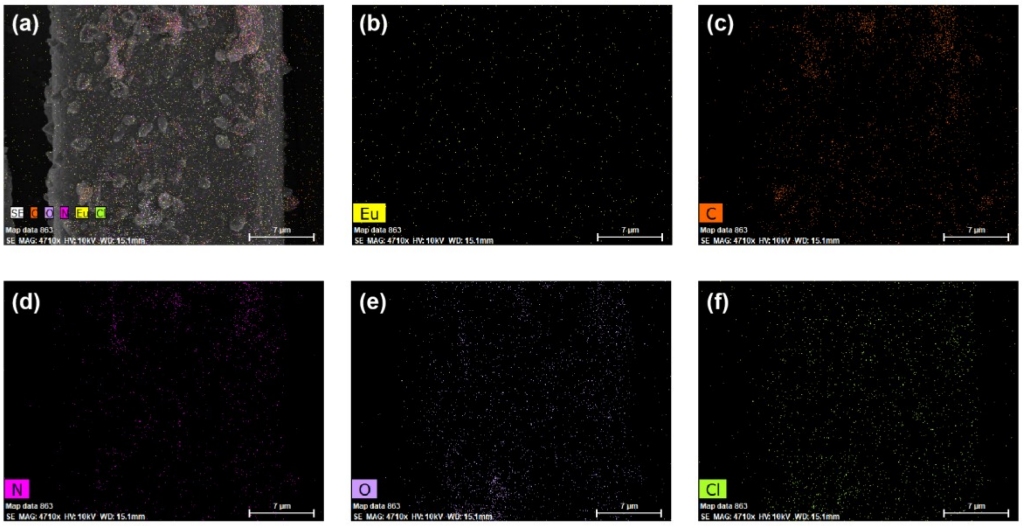


**Fig. S26.** (a−f) EDX mapping of Eu, C, N, O and C; elements for **1-HCl**.

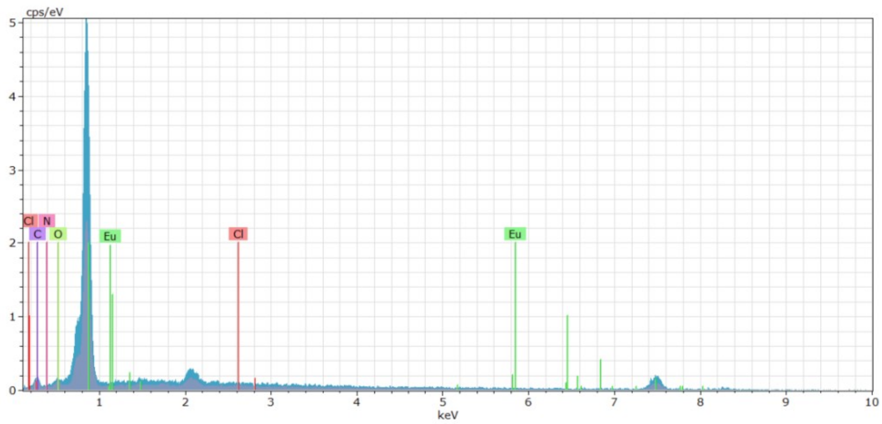


**Fig. S27.** EDS spectrum of **1-TFc**, involving the atom contents of Eu, C, N, O and Cl.

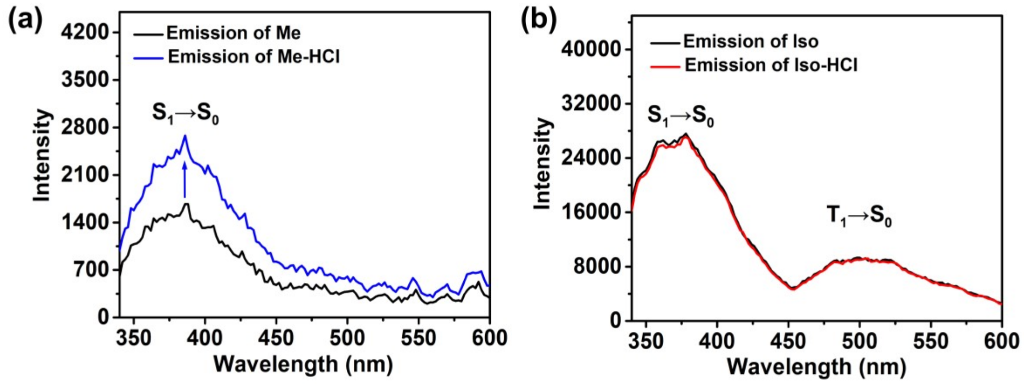


**Fig. S28.** (a) Emission spectra of Me and Me-HCl ($\lambda_{ex}$ = 292 nm). (b) Emission spectra of Iso and Iso-HCl ($\lambda_{ex}$ = 292 nm).

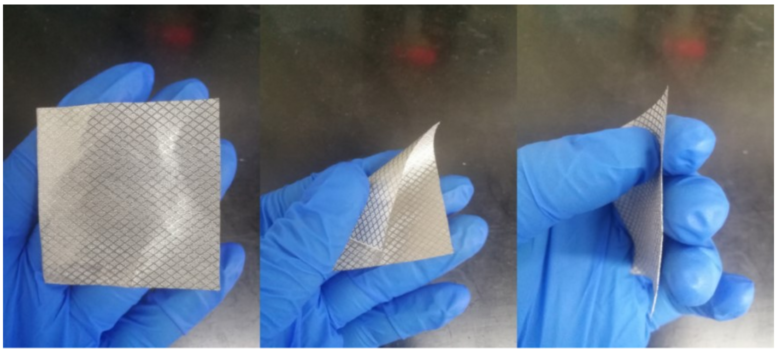

**Fig. S29.** The pictures of the flexible Cu/Ni conductive fabric.

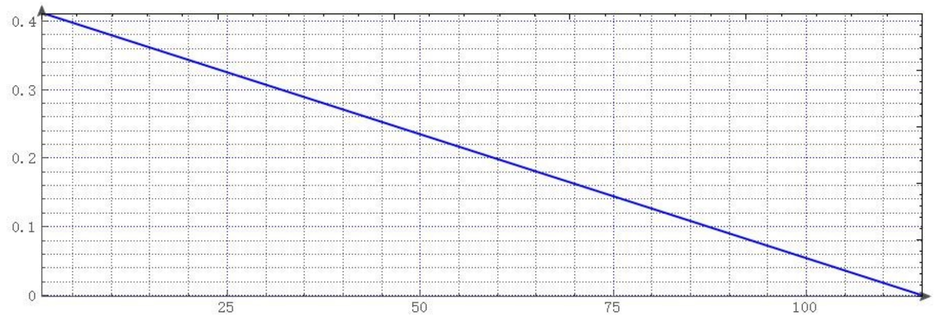

**Fig. S30.** The BPNN 1 training curve.

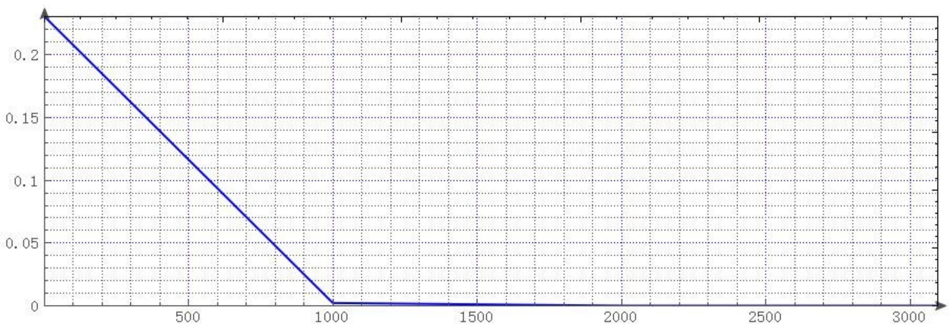

**Fig. S31.** The BPNN 2 training curve.

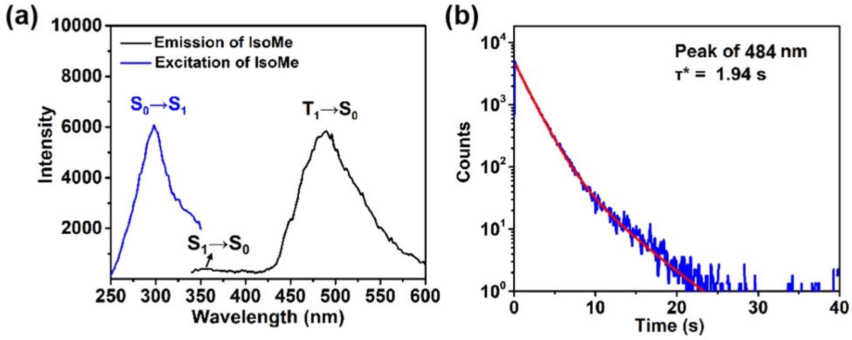


**Fig. S32.** (a) Emission and excitation spectra of IsoMe. (b) Phosphorescence lifetime curve of IsoMe by monitoring 488 nm emission peak.

**Table S1.** Summary of phosphorescence decay lifetime of **1**, **1-Eme**, **1-Nme**, **1-Mme**, **1-Ede**, **1-TFc** and **1-HCl**.

| Sample | $\lambda_{ex}$ (nm) | $\lambda_{em}$ (nm) | $\tau_1$ (ms) | $A_1$ | Percentage (%) | $\tau_2$ (ms) | $A_2$ | Percentage (%) | $\tau^*$ | $\chi^2$ |
|---|---|---|---|---|---|---|---|---|---|---|
| **1** | 292 | 484 | 819.48 | 2009.31 | 56.14 | 1550.45 | 829.71 | 43.86 | 1140.08 | 1.804 |
| **1-Eme** | 292 | 484 | 476.02 | 542.54 | 100.00 | | | | | 1.434 |
| **1-Nme** | 292 | 484 | 543.56 | 714.74 | 100.00 | | | | | 1.634 |
| **1-Mme** | 292 | 484 | 1029.62 | 935.96 | 100.00 | | | | | 1.815 |
| **1-Ede** | 292 | 484 | 595.84 | 63.99 | 100.00 | | | | | 1.229 |
| **1-TFc** | 292 | 484 | 393.47 | 187.89 | 7.32 | 1163.78 | 804.60 | 92.68 | 1075.66 | 1.522 |
| **1-HCl** | 292 | 484 | 594.05 | 63.79 | 100.00 | | | | | 1.333 |
| **IsoMe** | 292 | 484 | 1330.17 | 3933.56 | 65.69 | 3251.42 | 696.31 | 34.31 | 1940.2 | 1.231 |

[$\tau^* = (A_1\tau_1^2+A_2\tau_2^2)/(A_1\tau_1+A_2\tau_2)$]

**Table S2.** Summary of PL decay lifetime of **1**, **1-Eme**, **1-Nme**, **1-Mme**, **1-Ede**, **1-TFc** and **1-HCl**.

| Sample | $\lambda_{ex}$ (nm) | $\lambda_{em}$ (nm) | $\tau_1$ (us) | $A_1$ | Percentage (%) | $\tau_2$ (s) | $A_2$ | Percentage (%) | $\tau^*$ | $\chi^2$ |
|---|---|---|---|---|---|---|---|---|---|---|
| **1** | 292 | 615 | 261.80 | 1047.54 | 100.00 | | | | | 1.000 |
| **1-Eme** | 292 | 615 | 247.85 | 559.84 | 33.23 | 607.37 | 459.08 | 66.77 | 487.91 | 1.329 |
| **1-Nme** | 292 | 615 | 246.01 | 539.09 | 31.32 | 595.40 | 488.50 | 68.68 | 485.97 | 1.634 |
| **1-Mme** | 292 | 615 | 199.08 | 584.37 | 31.09 | 593.82 | 434.23 | 68.91 | 471.09 | 1.274 |
| **1-Ede** | 292 | 615 | 251.46 | 1310.63 | 35.66 | 752.77 | 789.82 | 64.34 | 573.99 | 1.023 |
| **1-TFc** | 292 | 615 | 216.11 | 903.07 | 50.06 | 471.71 | 101.17 | 49.94 | 266.10 | 1.243 |
| **1-HCl** | 292 | 615 | 3.24 | 11420.58 | 42.53 | 166.74 | 299.66 | 57.47 | 97.17 | 1.191 |

[$\tau^* = (A_1\tau_1^2+A_2\tau_2^2)/(A_1\tau_1+A_2\tau_2)$]

**Table S3.** CIE coordinates of **1** under various excitation from 250 to 400 nm.

| Excitation | x | y | Excitation | x | y |
|---|---|---|---|---|---|
| 250 | 0.3841 | 0.3266 | 330 | 0.2275 | 0.215 |
| 260 | 0.4035 | 0.3275 | 340 | 0.2146 | 0.1862 |
| 270 | 0.4039 | 0.3267 | 350 | 0.2056 | 0.1355 |
| 280 | 0.4159 | 0.327 | 360 | 0.2062 | 0.1214 |
| 290 | 0.4188 | 0.3262 | 370 | 0.191 | 0.1175 |
| 300 | 0.4524 | 0.3202 | 380 | 0.2681 | 0.2056 |
| 310 | 0.3735 | 0.283 | 390 | 0.2247 | 0.203 |

| | | | | | |
|---|---|---|---|---|---|
| 320 | 0.2595 | 0.2407 | 400 | 0.2945 | 0.2422 |

**Table S4.** Summary of input and output information during the training of BPNN 1 for classifying six LVCs and blank.

| Input (R.G.B value) | | | Output data (test objects) | | | | | | |
|---|---|---|---|---|---|---|---|---|---|
| $(I - I_0)/I_0$ | $\tau_{PL}$ | $\tau_P$ | Nme | Eme | Mme | Ede | TFc | HCl | Blank |
| 0.405 | 487.91 | 476.02 | 1 | 0 | 0 | 0 | 0 | 0 | 0 |
| 0.665 | 485.97 | 543.56 | 0 | 1 | 0 | 0 | 0 | 0 | 0 |
| 1.108 | 471.09 | 1029.62 | 0 | 0 | 1 | 0 | 0 | 0 | 0 |
| 2.81 | 573.99 | 595.84 | 0 | 0 | 0 | 1 | 0 | 0 | 0 |
| -0.162 | 266.1 | 393.47 | 0 | 0 | 0 | 0 | 1 | 0 | 0 |
| -0.674 | 97.17 | 594.05 | 0 | 0 | 0 | 0 | 0 | 1 | 0 |
| 0 | 261.8 | 1140.08 | 0 | 0 | 0 | 0 | 0 | 0 | 1 |

In Table S4, all data is used to training the BPNN 1. The $(I - I_0)/I_0$, $\tau_{PL}$ and $\tau_P$ values of **1-Nme**, **1-Eme**, **1-Mme**, **1-Ede**, **1-TFc**, **1-HCl** and **1** as input information are inputted in the input column of the BPNN. Various “0” and “1” inputted into the output column of the BPNN, in which “0” represents the false test object, and “1” represents the correct test object. All data is used to train the BPNN 1.

**Table S5.** Network structure information of BPNN 1.

| Network structure information | | | | |
|---|---|---|---|---|
| Input layer | 3 neurons | 1 Paranoid | | |
| Hidden layer 1 | 5 neurons | 1 Paranoid | | |
| Hidden layer 2 | 6 neurons | 1 Paranoid | | |
| Output layer | 7 neurons | | | |
| Network type | FANN_NETTYPE_LAYER | | | |
| Training function | FANN_TRAIN_RPROP | | | |
| Error function | FANN_ERRORFUNC_LINEAR | | | |
| Termination function | FANN_STOPFUNC_MSE | | | |
| Hidden layer excitation function | FANN_SIGMOID_SYMMETRIC | | | |
| Output layer excitation function | FANN_SIGMOID_SYMMETRIC | | | |
| **Network weight value** | | | | |
| Arrangement | Wire number | Output point (n) | Input point (m) | Weight value ($W$) |
| 1 | 0 | 0 | 4 | 1.10505 |
| | 1 | 1 | 4 | 2.12914 |
| | 2 | 2 | 4 | 0.548921 |
| | 3 | 3 | 4 | 0.594116 |
| | 4 | 0 | 5 | 1.89517 |
| | 5 | 1 | 5 | 1.73458 |
| | 6 | 2 | 5 | 1.3717 |
| | 7 | 3 | 5 | -0.266689 |

| | | | | |
|---|---|---|---|---|
| | 8 | 0 | 6 | 2.53372 |
| | 9 | 1 | 6 | 0.278359 |
| | 10 | 2 | 6 | 0.0674679 |
| | 11 | 3 | 6 | 0.69116 |
| | 12 | 0 | 7 | -0.620052 |
| | 13 | 1 | 7 | 0.857591 |
| | 14 | 2 | 7 | 2.88918 |
| | 15 | 3 | 7 | 1.34636 |
| | 16 | 0 | 8 | 1.49494 |
| | 17 | 1 | 8 | -2.21909 |
| | 18 | 2 | 8 | 1.52444 |
| | 19 | 3 | 8 | 1.65937 |
| | 20 | 4 | 10 | 0.241452 |
| | 21 | 5 | 10 | 1.02473 |
| | 22 | 6 | 10 | -3.00139 |
| | 23 | 7 | 10 | 2.78147 |
| | 24 | 8 | 10 | 0.424472 |
| | 25 | 9 | 10 | -0.0287807 |
| | 26 | 4 | 11 | -0.219319 |
| | 27 | 5 | 11 | 1.03912 |
| | 28 | 6 | 11 | 0.370994 |
| | 29 | 7 | 11 | 0.237197 |
| | 30 | 8 | 11 | 3.82317 |
| | 31 | 9 | 11 | 1.31334 |
| | 32 | 4 | 12 | 1.98588 |
| | 33 | 5 | 12 | 1.21297 |
| | 34 | 6 | 12 | 29.3638 |
| | 35 | 7 | 12 | 4.67511 |
| 2 | 36 | 8 | 12 | 0.587711 |
| | 37 | 9 | 12 | -0.282918 |
| | 38 | 4 | 13 | -0.273239 |
| | 39 | 5 | 13 | 2.69121 |
| | 40 | 6 | 13 | -1.40221 |
| | 41 | 7 | 13 | -90.5064 |
| | 42 | 8 | 13 | -36.3222 |
| | 43 | 9 | 13 | -553.569 |
| | 44 | 4 | 14 | 1.48272 |
| | 45 | 5 | 14 | 0.762762 |
| | 46 | 6 | 14 | -0.337677 |
| | 47 | 7 | 14 | 11.2883 |
| | 48 | 8 | 14 | -0.276754 |
| | 49 | 9 | 14 | 1.65234 |
| | 50 | 4 | 15 | 0.651955 |
| | 51 | 5 | 15 | 2.24245 |

| | | | | |
|---|---|---|---|---|
| | 52 | 6 | 15 | -0.532953 |
| | 53 | 7 | 15 | 0.598986 |
| | 54 | 8 | 15 | -1.01524 |
| | 55 | 9 | 15 | -5.35487 |
| | 56 | 10 | 17 | 11.1918 |
| | 57 | 11 | 17 | -34.3962 |
| | 58 | 12 | 17 | -6.18197 |
| | 59 | 13 | 17 | 2.27025 |
| | 60 | 14 | 17 | 0.445497 |
| | 61 | 15 | 17 | 5.43375 |
| | 62 | 16 | 17 | -5.85281 |
| | 63 | 10 | 18 | 0.65994 |
| | 64 | 11 | 18 | -38.8956 |
| | 65 | 12 | 18 | 29.3379 |
| | 66 | 13 | 18 | 18.0049 |
| | 67 | 14 | 18 | 8.53059 |
| | 68 | 15 | 18 | 0.0529693 |
| | 69 | 16 | 18 | -5.50438 |
| | 70 | 10 | 19 | 1500 |
| | 71 | 11 | 19 | 620.194 |
| | 72 | 12 | 19 | 1500 |
| | 73 | 13 | 19 | 1500 |
| | 74 | 14 | 19 | 986.717 |
| 3 | 75 | 15 | 19 | 1500 |
| | 76 | 16 | 19 | 756.246 |
| | 77 | 10 | 20 | -38.346 |
| | 78 | 11 | 20 | 31.2211 |
| | 79 | 12 | 20 | 9.63353 |
| | 80 | 13 | 20 | 11.8137 |
| | 81 | 14 | 20 | -0.320654 |
| | 82 | 15 | 20 | 10.8448 |
| | 83 | 16 | 20 | -10.986 |
| | 84 | 10 | 21 | -25.7457 |
| | 85 | 11 | 21 | -6.70965 |
| | 86 | 12 | 21 | 1.11416 |
| | 87 | 13 | 21 | 3.09921 |
| | 88 | 14 | 21 | -22.8434 |
| | 89 | 15 | 21 | 1.93863 |
| | 90 | 16 | 21 | -4.21398 |
| | 91 | 10 | 22 | 5.55457 |
| | 92 | 11 | 22 | 24.7463 |
| | 93 | 12 | 22 | 0.5815 |
| | 94 | 13 | 22 | 8.93692 |
| | 95 | 14 | 22 | -17.4828 |

| | | | | |
|---|---|---|---|---|
| | 96 | 15 | 22 | 0.643751 |
| | 97 | 16 | 22 | -14.6922 |
| | 98 | 10 | 23 | 16.9898 |
| | 99 | 11 | 23 | 0.877639 |
| | 100 | 12 | 23 | -14.8437 |
| | 101 | 13 | 23 | 3.52038 |
| | 102 | 14 | 23 | 15.3328 |
| | 103 | 15 | 23 | 16.407 |
| | 104 | 16 | 23 | -12.4436 |
| Input / output column coefficients for manual calculation | | | | |
| Listing | Minimum | Maximum | | |
| $(I - I_0)/I_0$ | -0.709474 | 2.95789 | | |
| $\tau_{PL}$ | 92.3115 | 604.2 | | |
| $\tau_P$ | 373.796 | 1200.08 | | |
| Nme | 0 | 1 | | |
| Eme | 0 | 1 | | |
| Mme | 0 | 1 | | |
| Ede | 0 | 1 | | |
| TFc | 0 | 1 | | |
| HCl | 0 | 1 | | |
| Blank | 0 | 1 | | |
| Deviation statistics: mean variance | | | | |
| Listing | All rows | Calculation line | Test line | |
| Nme | 4.72857e-11 | 4.72857e-11 | 0 | |
| Eme | 0 | 0 | 0 | |
| Mme | 0 | 0 | 0 | |
| Ede | 0 | 0 | 0 | |
| TFc | 6.42857e-13 | 6.42857e-13 | 0 | |
| HCl | 2.96429e-11 | 2.96429e-11 | 0 | |
| Blank | 2.85714e-13 | 2.85714e-13 | 0 | |

**Table S6.** The summary of mean square error (MSE), original value (OV), calculated value (CV), variance (Var.) for BPNN 1.

| 1 | Input item | | | Nme (MSE = 4.72857e-11) | | | Eme (MSE = 0) | | | Mme (MSE = 0) | | | Ede (MSE = 0) | | |
|---|---|---|---|---|---|---|---|---|---|---|---|---|---|---|---|
| 2 | $(I - I_0)/I_0$ | $\tau_{PL}$ | $\tau_P$ | OV. | CV. | Var. | OV. | CV. | Var. | OV. | CV. | Var. | OV. | CV. | Var. |
| 3 | 0.405 | 487.91 | 476.02 | 1 | 0.999991 | 8.1e-11 | 0 | 0 | 0 | 0 | 0 | 0 | 0 | 0 | 0 |
| 4 | 0.665 | 485.97 | 543.56 | 0 | 9e-06 | 8.1e-11 | 1 | 1 | 0 | 0 | 0 | 0 | 0 | 0 | 0 |
| 5 | 1.108 | 471.09 | 1029.62 | 0 | 0 | 0 | 0 | 0 | 0 | 1 | 1 | 0 | 0 | 0 | 0 |
| 6 | 2.81 | 573.99 | 595.84 | 0 | 0 | 0 | 0 | 0 | 0 | 0 | 0 | 0 | 1 | 1 | 0 |
| 7 | -0.162 | 266.1 | 393.47 | 0 | 1.3e-05 | 1.69e-10 | 0 | 0 | 0 | 0 | 0 | 0 | 0 | 0 | 0 |
| 8 | -0.674 | 97.17 | 594.05 | 0 | 0 | 0 | 0 | 0 | 0 | 0 | 0 | 0 | 0 | 0 | 0 |
| 9 | 0 | 261.8 | 1140.08 | 0 | 0 | 0 | 0 | 0 | 0 | 0 | 0 | 0 | 0 | 0 | 0 |

| 1 | TFc (MSE = 6.42857e-13) | | | HCl (MSE = 2.96429e-11) | | | Blank (MSE = 2.85714e-13) | | |
|---|---|---|---|---|---|---|---|---|---|
| 2 | OV. | CV. | Var. | OV. | CV. | Var. | OV. | CV. | Var. |
| 3 | 0 | 1.5e-06 | 2.25e-12 | 0 | 0 | 0 | 0 | 1e-06 | 1e-12 |
| 4 | 0 | 0 | 0 | 0 | 0 | 0 | 0 | 0 | 0 |
| 5 | 0 | 0 | 0 | 0 | 4.5e-06 | 2.025e-11 | 0 | 0 | 0 |
| 6 | 0 | 0 | 0 | 0 | 0 | 0 | 0 | 0 | 0 |
| 7 | 1 | 1 | 0 | 0 | 1e-05 | 1e-10 | 0 | 0 | 0 |
| 8 | 0 | 1.5e-06 | 2.25e-12 | 1 | 0.999991 | 8.1e-11 | 0 | 0 | 0 |
| 9 | 0 | 0 | 0 | 0 | 2.5e-06 | 6.25e-12 | 1 | 0.999999 | 1e-12 |

In Table S6, all data is utilized to test the BPNN 1. The $(I - I_0)/I_0$, $\tau_{PL}$ and $\tau_P$ values of **1-Nme**, **1-Eme**, **1-Mme**, **1-Ede**, **1-TFc**, **1-HCl** and **1** as input information are inputted in the input column of the BPNN 1. Through the BPNN 1 calculation, various values (0-1) can be outputted, in which the values close to "0" represents the false test object, the values close to "1" represents the correct test object. By comparing the OV with CV, the variance can be obtained, which suggests that the BPNN 1 has a good accuracy for classifying six LVCs.

**Table S7.** The summary of input and output information in real batch calculation during the test of BPNN 1.

| Input data | | | Output data | | | | | | |
|---|---|---|---|---|---|---|---|---|---|
| $(I - I_0)/I_0$ | $\tau_{PL}$ | $\tau_P$ | Nme | Eme | Mme | Ede | TFc | HCl | Blank |
| 0.405 | 487.91 | 476.02 | 0.999991 | 0 | 0 | 0 | 1.5e-06 | 0 | 1e-06 |
| 0.665 | 485.97 | 543.56 | 9e-06 | 1 | 0 | 0 | 0 | 0 | 0 |
| 1.108 | 471.09 | 1029.62 | 0 | 0 | 1 | 0 | 0 | 4.5e-06 | 0 |
| 2.81 | 573.99 | 595.84 | 0 | 0 | 0 | 1 | 0 | 0 | 0 |
| -0.162 | 266.1 | 393.47 | 1.3e-05 | 0 | 0 | 0 | 1 | 1e-05 | 0 |
| -0.674 | 97.17 | 594.05 | 0 | 0 | 0 | 0 | 1.5e-06 | 0.999991 | 0 |
| 0 | 261.8 | 1140.08 | 0 | 0 | 0 | 0 | 0 | 2.5e-06 | 0.999999 |

In Table S7, all data is utilized to test the BPNN 1. The $(I - I_0)/I_0$, $\tau_{PL}$ and $\tau_P$ values of **1-Nme**, **1-Eme**, **1-Mme**, **1-Ede**, **1-TFc**, **1-HCl** and **1** as input information are inputted in the input column of the BPNN 1. Through the BPNN calculation, various values (0-1) can be acquired, in which the values close to "0" represents the false test object, and the values close to 1 represents the correct test object.

**Table S8.** The matlab code of this BPNN 1.

**Matlab code**

```
function [fO0, fO1, fO2, fO3, fO4, fO5, fO6] = MPredict(fI0, fI1, fI2)
    fI0 = (fI0 - (-0.7094736842105264 + 2.9578947368421056 ) / 2.0) /(2.9578947368421056 - (-0.7094736842105264 + 2.9578947368421056 ) / 2.0);
    fI1 = (fI1 - (92.3114999999999952 + 604.2000000000000455 ) / 2.0) /(604.2000000000000455 - (92.3114999999999952 + 604.2000000000000455 ) / 2.0);
    fI2 = (fI2 - (373.7964999999999804 + 1200.0842105263157009 ) / 2.0) /(1200.0842105263157009 - (373.7964999999999804 + 1200.0842105263157009 ) / 2.0);
    fWei0 = 1.10505;
    fWei1 = 2.12914;
    fWei2 = 0.548921;
    fWei3 = 0.594116;
    fWei4 = 1.89517;
    fWei5 = 1.73458;
    fWei6 = 1.3717;
```

```
fWei7 = -0.266689;
fWei8 = 2.53372;
fWei9 = 0.278359;
fWei10 = 0.0674679;
fWei11 = 0.69116;
fWei12 = -0.620052;
fWei13 = 0.857591;
fWei14 = 2.88918;
fWei15 = 1.34636;
fWei16 = 1.49494;
fWei17 = -2.21909;
fWei18 = 1.52444;
fWei19 = 1.65937;
fWei20 = 0.241452;
fWei21 = 1.02473;
fWei22 = -3.00139;
fWei23 = 2.78147;
fWei24 = 0.424472;
fWei25 = -0.0287807;
fWei26 = -0.219319;
fWei27 = 1.03912;
fWei28 = 0.370994;
fWei29 = 0.237197;
fWei30 = 3.82317;
fWei31 = 1.31334;
fWei32 = 1.98588;
fWei33 = 1.21297;
fWei34 = 29.3638;
fWei35 = 4.67511;
fWei36 = 0.587711;
fWei37 = -0.282918;
fWei38 = -0.273239;
fWei39 = 2.69121;
fWei40 = -1.40221;
fWei41 = -90.5064;
fWei42 = -36.3222;
fWei43 = -553.569;
fWei44 = 1.48272;
fWei45 = 0.762762;
fWei46 = -0.337677;
fWei47 = 11.2883;
fWei48 = -0.276754;
fWei49 = 1.65234;
fWei50 = 0.651955;
fWei51 = 2.24245;
fWei52 = -0.532953;
fWei53 = 0.598986;
fWei54 = -1.01524;
fWei55 = -5.35487;
fWei56 = 11.1918;
fWei57 = -34.3962;
fWei58 = -6.18197;
fWei59 = 2.27025;
fWei60 = 0.445497;
fWei61 = 5.43375;
fWei62 = -5.85281;
fWei63 = 0.65994;
fWei64 = -38.8956;
fWei65 = 29.3379;
fWei66 = 18.0049;
fWei67 = 8.53059;
fWei68 = 0.0529693;
fWei69 = -5.50438;
fWei70 = 1500;
fWei71 = 620.194;
fWei72 = 1500;
fWei73 = 1500;
fWei74 = 986.717;
fWei75 = 1500;
```

```
fWei76 = 756.246;
fWei77 = -38.346;
fWei78 = 31.2211;
fWei79 = 9.63353;
fWei80 = 11.8137;
fWei81 = -0.320654;
fWei82 = 10.8448;
fWei83 = -10.986;
fWei84 = -25.7457;
fWei85 = -6.70965;
fWei86 = 1.11416;
fWei87 = 3.09921;
fWei88 = -22.8434;
fWei89 = 1.93863;
fWei90 = -4.21398;
fWei91 = 5.55457;
fWei92 = 24.7463;
fWei93 = 0.5815;
fWei94 = 8.93692;
fWei95 = -17.4828;
fWei96 = 0.643751;
fWei97 = -14.6922;
fWei98 = 16.9898;
fWei99 = 0.877639;
fWei100 = -14.8437;
fWei101 = 3.52038;
fWei102 = 15.3328;
fWei103 = 16.407;
fWei104 = -12.4436;
f0 = fI0;
f1 = fI1;
f2 = fI2;
f3 = 1.0;
f4 = 0.0;
f5 = 0.0;
f6 = 0.0;
f7 = 0.0;
f8 = 0.0;
f4 = f4 + f0 * fWei0;
f4 = f4 + f1 * fWei1;
f4 = f4 + f2 * fWei2;
f4 = f4 + f3 * fWei3;
f4 = f4 * 0.5;
f4 = (2.0 / (1.0 + exp(-2.0 * f4))- 1.0);
f5 = f5 + f0 * fWei4;
f5 = f5 + f1 * fWei5;
f5 = f5 + f2 * fWei6;
f5 = f5 + f3 * fWei7;
f5 = f5 * 0.5;
f5 = (2.0 / (1.0 + exp(-2.0 * f5))- 1.0);
f6 = f6 + f0 * fWei8;
f6 = f6 + f1 * fWei9;
f6 = f6 + f2 * fWei10;
f6 = f6 + f3 * fWei11;
f6 = f6 * 0.5;
f6 = (2.0 / (1.0 + exp(-2.0 * f6))- 1.0);
f7 = f7 + f0 * fWei12;
f7 = f7 + f1 * fWei13;
f7 = f7 + f2 * fWei14;
f7 = f7 + f3 * fWei15;
f7 = f7 * 0.5;
f7 = (2.0 / (1.0 + exp(-2.0 * f7))- 1.0);
f8 = f8 + f0 * fWei16;
f8 = f8 + f1 * fWei17;
f8 = f8 + f2 * fWei18;
f8 = f8 + f3 * fWei19;
f8 = f8 * 0.5;
f8 = (2.0 / (1.0 + exp(-2.0 * f8))- 1.0);
f9 = 1.0;
```

```
f10 = 0.0;
f11 = 0.0;
f12 = 0.0;
f13 = 0.0;
f14 = 0.0;
f15 = 0.0;
f10 = f10 + f4 * fWei20;
f10 = f10 + f5 * fWei21;
f10 = f10 + f6 * fWei22;
f10 = f10 + f7 * fWei23;
f10 = f10 + f8 * fWei24;
f10 = f10 + f9 * fWei25;
f10 = f10 * 0.5;
f10 = (2.0 / (1.0 + exp(-2.0 * f10))- 1.0);
f11 = f11 + f4 * fWei26;
f11 = f11 + f5 * fWei27;
f11 = f11 + f6 * fWei28;
f11 = f11 + f7 * fWei29;
f11 = f11 + f8 * fWei30;
f11 = f11 + f9 * fWei31;
f11 = f11 * 0.5;
f11 = (2.0 / (1.0 + exp(-2.0 * f11))- 1.0);
f12 = f12 + f4 * fWei32;
f12 = f12 + f5 * fWei33;
f12 = f12 + f6 * fWei34;
f12 = f12 + f7 * fWei35;
f12 = f12 + f8 * fWei36;
f12 = f12 + f9 * fWei37;
f12 = f12 * 0.5;
f12 = (2.0 / (1.0 + exp(-2.0 * f12))- 1.0);
f13 = f13 + f4 * fWei38;
f13 = f13 + f5 * fWei39;
f13 = f13 + f6 * fWei40;
f13 = f13 + f7 * fWei41;
f13 = f13 + f8 * fWei42;
f13 = f13 + f9 * fWei43;
f13 = f13 * 0.5;
f13 = (2.0 / (1.0 + exp(-2.0 * f13))- 1.0);
f14 = f14 + f4 * fWei44;
f14 = f14 + f5 * fWei45;
f14 = f14 + f6 * fWei46;
f14 = f14 + f7 * fWei47;
f14 = f14 + f8 * fWei48;
f14 = f14 + f9 * fWei49;
f14 = f14 * 0.5;
f14 = (2.0 / (1.0 + exp(-2.0 * f14))- 1.0);
f15 = f15 + f4 * fWei50;
f15 = f15 + f5 * fWei51;
f15 = f15 + f6 * fWei52;
f15 = f15 + f7 * fWei53;
f15 = f15 + f8 * fWei54;
f15 = f15 + f9 * fWei55;
f15 = f15 * 0.5;
f15 = (2.0 / (1.0 + exp(-2.0 * f15))- 1.0);
f16 = 1.0;
f17 = 0.0;
f18 = 0.0;
f19 = 0.0;
f20 = 0.0;
f21 = 0.0;
f22 = 0.0;
f23 = 0.0;
f17 = f17 + f10 * fWei56;
f17 = f17 + f11 * fWei57;
f17 = f17 + f12 * fWei58;
f17 = f17 + f13 * fWei59;
f17 = f17 + f14 * fWei60;
f17 = f17 + f15 * fWei61;
f17 = f17 + f16 * fWei62;
```

```
f17 = f17 * 0.5;
f17 = (2.0 / (1.0 + exp(-2.0 * f17))- 1.0);
f18 = f18 + f10 * fWei63;
f18 = f18 + f11 * fWei64;
f18 = f18 + f12 * fWei65;
f18 = f18 + f13 * fWei66;
f18 = f18 + f14 * fWei67;
f18 = f18 + f15 * fWei68;
f18 = f18 + f16 * fWei69;
f18 = f18 * 0.5;
f18 = (2.0 / (1.0 + exp(-2.0 * f18))- 1.0);
f19 = f19 + f10 * fWei70;
f19 = f19 + f11 * fWei71;
f19 = f19 + f12 * fWei72;
f19 = f19 + f13 * fWei73;
f19 = f19 + f14 * fWei74;
f19 = f19 + f15 * fWei75;
f19 = f19 + f16 * fWei76;
f19 = f19 * 0.5;
f19 = (2.0 / (1.0 + exp(-2.0 * f19))- 1.0);
f20 = f20 + f10 * fWei77;
f20 = f20 + f11 * fWei78;
f20 = f20 + f12 * fWei79;
f20 = f20 + f13 * fWei80;
f20 = f20 + f14 * fWei81;
f20 = f20 + f15 * fWei82;
f20 = f20 + f16 * fWei83;
f20 = f20 * 0.5;
f20 = (2.0 / (1.0 + exp(-2.0 * f20))- 1.0);
f21 = f21 + f10 * fWei84;
f21 = f21 + f11 * fWei85;
f21 = f21 + f12 * fWei86;
f21 = f21 + f13 * fWei87;
f21 = f21 + f14 * fWei88;
f21 = f21 + f15 * fWei89;
f21 = f21 + f16 * fWei90;
f21 = f21 * 0.5;
f21 = (2.0 / (1.0 + exp(-2.0 * f21))- 1.0);
f22 = f22 + f10 * fWei91;
f22 = f22 + f11 * fWei92;
f22 = f22 + f12 * fWei93;
f22 = f22 + f13 * fWei94;
f22 = f22 + f14 * fWei95;
f22 = f22 + f15 * fWei96;
f22 = f22 + f16 * fWei97;
f22 = f22 * 0.5;
f22 = (2.0 / (1.0 + exp(-2.0 * f22))- 1.0);
f23 = f23 + f10 * fWei98;
f23 = f23 + f11 * fWei99;
f23 = f23 + f12 * fWei100;
f23 = f23 + f13 * fWei101;
f23 = f23 + f14 * fWei102;
f23 = f23 + f15 * fWei103;
f23 = f23 + f16 * fWei104;
f23 = f23 * 0.5;
f23 = (2.0 / (1.0 + exp(-2.0 * f23))- 1.0);
fO0 = f17;
fO1 = f18;
fO2 = f19;
fO3 = f20;
fO4 = f21;
fO5 = f22;
fO6 = f23;
fO0 = fO0 * (1 - (0 + 1 ) / 2.0) + (0 + 1) / 2.0;
fO1 = fO1 * (1 - (0 + 1 ) / 2.0) + (0 + 1) / 2.0;
fO2 = fO2 * (1 - (0 + 1 ) / 2.0) + (0 + 1) / 2.0;
fO3 = fO3 * (1 - (0 + 1 ) / 2.0) + (0 + 1) / 2.0;
fO4 = fO4 * (1 - (0 + 1 ) / 2.0) + (0 + 1) / 2.0;
fO5 = fO5 * (1 - (0 + 1 ) / 2.0) + (0 + 1) / 2.0;
```

```
fO6 = fO6 * (1 - (0 + 1 ) / 2.0) + (0 + 1) / 2.0;
```

**Table S9.** Summary of fluorescence sensing parameters of **1** for detecting **Nme**, **Eme**, **Mme**, **Ede**, **TFc** and **HCl**.

| LVCs | Nme | Eme | Mme | Ede |
|---|---|---|---|---|
| Concentration range (ppm) | 100−600 | 100−600 | 100−600 | 100−600 |
| Linear relationship | $I = 15.7c + 22650$ | $I = 5.8c + 3870$ | $I = 9.52c + 3878$ | $I = 47.97c + 11667$ |
| Correlation coefficient ($R^2$) | 0.992 | 0.994 | 0.994 | 0.993 |
| Detection limit (DL) | 34.23 ppm | 25.34 ppm | 11.65 ppm | 4.74 ppm |
| Response time (s) | 12 | 11 | 12 | 9 |
| Cycle times | 6 | 5 | 6 | 4 |
| **LVCs** | **TFc** | **HCl** | | |
| Concentration range (ppm) | 100−600 | 100−600 | | |
| Linear relationship | $I = -16.1c + 13878$ | $I = -48.26c + 29225.8$ | | |
| Correlation coefficient ($R^2$) | 0.995 | 0.997 | | |
| Detection limit (DL) | 12.62 ppm | 2.54 ppm | | |
| Response time (s) | 4 | 3 | | |
| Cycle times | 5 | 5 | | |

**Table S10.** Summary of input and output information during the training of BPNN 2 for recognizing the concentration of **Nme**.

| Input (R.G.B value) | Output data (Concentration of Nme) | | | | | |
|---|---|---|---|---|---|---|
| $I_{615}/I_{484}$ | 100 ppm | 200 ppm | 300 ppm | 400 ppm | 500 ppm | 600 ppm |
| 9.756 | 1 | 0 | 0 | 0 | 0 | 0 |
| 12.321 | 0 | 1 | 0 | 0 | 0 | 0 |
| 16.035 | 0 | 0 | 1 | 0 | 0 | 0 |
| 21.893 | 0 | 0 | 0 | 1 | 0 | 0 |
| 32.509 | 0 | 0 | 0 | 0 | 1 | 0 |
| 57.63 | 0 | 0 | 0 | 0 | 0 | 1 |

In Table S10, all data is used to training the BPNN 2. The $I_{615}/I_{484}$ values of every concentration as input information are inputted in the input column of the BPNN 2. Various “0” and “1” inputted into the output column of the BPNN 2, in which “0” represents the false concentration, and “1” represents the correct concentration. All data is used to train the BPNN 2.

**Table S11.** Network structure information of BPNN 2.

| Network structure information | | | | |
|---|---|---|---|---|
| Input layer | 1 neurons | 1 Paranoid | | |
| Hidden layer 1 | 6 neurons | 1 Paranoid | | |
| Output layer | 6 neurons | | | |
| Network type | FANN_NETTYPE_LAYER | | | |
| Training function | FANN_TRAIN_RPROP | | | |
| Error function | FANN_ERRORFUNC_LINEAR | | | |
| Termination function | FANN_STOPFUNC_MSE | | | |
| Hidden layer excitation function | FANN_SIGMOID_SYMMETRIC | | | |
| Output layer excitation function | FANN_SIGMOID_SYMMETRIC | | | |
| **Network weight value** | | | | |
| Arrangement | Wire number | Output point (n) | Input point (m) | Weight value (*W*) |
| | 0 | 0 | 2 | 13.4965 |
| | 1 | 1 | 2 | 8.5918 |
| | 2 | 0 | 3 | 1500 |
| | 3 | 1 | 3 | -1500 |
| | 4 | 0 | 4 | 1500 |
| | 5 | 1 | 4 | -1500 |
| 1 | 6 | 0 | 5 | 3.20266 |
| | 7 | 1 | 5 | 2.37858 |
| | 8 | 0 | 6 | -9.7364 |
| | 9 | 1 | 6 | -6.43768 |
| | 10 | 0 | 7 | -0.0627362 |
| | 11 | 1 | 7 | -1.62085 |
| | 12 | 2 | 9 | 0.767244 |
| | 13 | 3 | 9 | 2.97964 |
| | 14 | 4 | 9 | 2.48638 |
| | 15 | 5 | 9 | -390.565 |
| | 16 | 6 | 9 | 162.721 |
| | 17 | 7 | 9 | 629.76 |
| | 18 | 8 | 9 | 163.872 |
| 2 | 19 | 2 | 10 | -23.3227 |
| | 20 | 3 | 10 | 10.0919 |
| | 21 | 4 | 10 | 8.38097 |
| | 22 | 5 | 10 | 204.567 |
| | 23 | 6 | 10 | 120.699 |
| | 24 | 7 | 10 | 60.7321 |
| | 25 | 8 | 10 | -7.57263 |
| | 26 | 2 | 11 | -240.193 |

| | | | | |
|---|---|---|---|---|
| | 27 | 3 | 11 | 2.92093 |
| | 28 | 4 | 11 | 4.84024 |
| | 29 | 5 | 11 | 135.699 |
| | 30 | 6 | 11 | -168.156 |
| | 31 | 7 | 11 | 97.1709 |
| | 32 | 8 | 11 | -0.886454 |
| | 33 | 2 | 12 | -46.5131 |
| | 34 | 3 | 12 | -52.9383 |
| | 35 | 4 | 12 | -52.9938 |
| | 36 | 5 | 12 | -373.813 |
| | 37 | 6 | 12 | -274.226 |
| | 38 | 7 | 12 | 248.597 |
| | 39 | 8 | 12 | 87.6538 |
| | 40 | 2 | 13 | 206.085 |
| | 41 | 3 | 13 | -65.1376 |
| | 42 | 4 | 13 | -17.3287 |
| | 43 | 5 | 13 | -77.1919 |
| | 44 | 6 | 13 | 10.2998 |
| | 45 | 7 | 13 | 356.934 |
| | 46 | 8 | 13 | 31.2925 |
| | 47 | 2 | 14 | 127.591 |
| | 48 | 3 | 14 | 254.148 |
| | 49 | 4 | 14 | 108.609 |
| | 50 | 5 | 14 | 87.0099 |
| | 51 | 6 | 14 | 5.66207 |
| | 52 | 7 | 14 | -218.754 |
| | 53 | 8 | 14 | 16.4265 |
| Input / output column coefficients for manual calculation | | | | |
| Listing | Minimum | Maximum | | |
| $I_{615}/I_{484}$ | 9.2682 | 60.6632 | | |
| 100 ppm | 0 | 1 | | |
| 200 ppm | 0 | 1 | | |
| 300 ppm | 0 | 1 | | |
| 400 ppm | 0 | 1 | | |
| 500 ppm | 0 | 1 | | |
| 600 ppm | 0 | 1 | | |
| Deviation statistics: mean variance | | | | |
| Listing | All rows | Calculation line | Test line | |
| 100 ppm | 0 | 0 | 0 | |
| 200 ppm | 5.40325e-07 | 5.40325e-07 | 0 | |
| 300 ppm | 6e-11 | 6e-11 | 0 | |
| 400 ppm | 0 | 0 | 0 | |
| 500 ppm | 8.70417e-11 | 8.70417e-11 | 0 | |
| 600 ppm | 8.68333e-11 | 8.68333e-11 | 0 | |

**Table S12.** The summary of mean square error (MSE), original value (OV), calculated value (CV), variance (Var.) of BPNN 2.

| 1 | Input item | 100 ppm (MSE = 0) | | | 200 ppm (MSE = 5.40325e-07) | | | 300 ppm (MSE = 6e-11) | | | 400 ppm (MSE = 0) | | |
|---|---|---|---|---|---|---|---|---|---|---|---|---|---|
| 2 | $I_{615}/I_{484}$ | OV. | CV. | Var. | OV. | CV. | Var. | OV. | CV. | Var. | OV. | CV. | Var. |
| 3 | 9.756 | 1 | 1 | 0 | 0 | 0.0010565 | 1.11619e-06 | 0 | 0 | 0 | 0 | 0 | 0 |
| 4 | 12.321 | 0 | 0 | 0 | 1 | 0.998605 | 1.94603e-06 | 0 | 1e-05 | 1e-10 | 0 | 0 | 0 |
| 5 | 16.035 | 0 | 0 | 0 | 0 | 0.0004145 | 1.7181e-07 | 1 | 0.999984 | 2.56e-10 | 0 | 0 | 0 |
| 6 | 21.893 | 0 | 0 | 0 | 0 | 0 | 0 | 0 | 0 | 0 | 1 | 1 | 0 |
| 7 | 32.509 | 0 | 0 | 0 | 0 | 0 | 0 | 0 | 0 | 0 | 0 | 0 | 0 |
| 8 | 57.63 | 0 | 0 | 0 | 0 | 8.9e-05 | 7.921e-09 | 0 | 2e-06 | 4e-12 | 0 | 0 | 0 |

| 1 | 500 ppm (MSE = 8.70417e-11) | | | 600 ppm (MSE = 8.68333e-11) | | |
|---|---|---|---|---|---|---|
| 2 | OV. | CV. | Var. | OV. | CV. | Var. |
| 3 | 0 | 0 | 0 | 0 | 0 | 0 |
| 4 | 0 | 0 | 0 | 0 | 0 | 0 |
| 5 | 0 | 0 | 0 | 0 | 0 | 0 |
| 6 | 0 | 4e-06 | 1.6e-11 | 0 | 0 | 0 |
| 7 | 1 | 0.999982 | 3.24e-10 | 0 | 2e-05 | 4e-10 |
| 8 | 0 | 1.35e-05 | 1.8225e-10 | 1 | 0.999989 | 1.21e-10 |

In Table S12, all data is utilized to test the BPNN 2. The $I_{615}/I_{484}$ values of every concentration as input information are inputted in the input column of the BPNN 2. Through the BPNN 2 calculation, various values (0-1) can be outputted, in which the values close to “0” represents the false concentration, the values close to “1” represents the correct concentration. By comparing the OV with CV, the variance can be obtained, which suggests that the BPNN 2 has a good accuracy for detecting concentration.

**Table S13.** The summary of input and output information in real batch calculation during the test of BPNN 2.

| Input item | Output data | | | | | |
|---|---|---|---|---|---|---|
| $I_{615}/I_{484}$ | 100 ppm | 200 ppm | 300 ppm | 400 ppm | 500 ppm | 600 ppm |
| 9.756 | 1 | 0.0010565 | 0 | 0 | 0 | 0 |
| 12.321 | 0 | 0.998605 | 1e-05 | 0 | 0 | 0 |
| 16.035 | 0 | 0.0004145 | 0.999984 | 0 | 0 | 0 |
| 21.893 | 0 | 0 | 0 | 1 | 4e-06 | 0 |
| 32.509 | 0 | 0 | 0 | 0 | 0.999982 | 2e-05 |

| | | | | | | |
|---|---|---|---|---|---|---|
| 57.63 | 0 | 8.9e-05 | 2e-06 | 0 | 1.35e-05 | 0.999989 |

In Table S13, all data is utilized to test the BPNN 2. The $I_{615}/I_{484}$ values of every concentration as input information are inputted in the input column of the BPNN 2. Through the BPNN 2 calculation, various values (0-1) can be acquired, in which the values close to “0” represents the false concentration, and the values close to 1 represents the correct concentration.

**Table S14.** The matlab code of this BPNN 2.

**Matlab code**

```
function [fO0, fO1, fO2, fO3, fO4, fO5] = MPredict(fI0)
    fI0 = (fI0 - (9.2682000000000002 + 60.6631578947368482 ) / 2.0) /(60.6631578947368482 - (9.2682000000000002 + 60.6631578947368482 ) / 2.0);
    fWei0 = 13.4965;
    fWei1 = 8.5918;
    fWei2 = 1500;
    fWei3 = -1500;
    fWei4 = 1500;
    fWei5 = -1500;
    fWei6 = 3.20266;
    fWei7 = 2.37858;
    fWei8 = -9.7364;
    fWei9 = -6.43768;
    fWei10 = -0.0627362;
    fWei11 = -1.62085;
    fWei12 = 0.767244;
    fWei13 = 2.97964;
    fWei14 = 2.48638;
    fWei15 = -390.565;
    fWei16 = 162.721;
    fWei17 = 629.76;
    fWei18 = 163.872;
    fWei19 = -23.3227;
    fWei20 = 10.0919;
    fWei21 = 8.38097;
    fWei22 = 204.567;
    fWei23 = 120.699;
    fWei24 = 60.7321;
    fWei25 = -7.57263;
    fWei26 = -240.193;
    fWei27 = 2.92093;
    fWei28 = 4.84024;
    fWei29 = 135.699;
    fWei30 = -168.156;
    fWei31 = 97.1709;
    fWei32 = -0.886454;
    fWei33 = -46.5131;
    fWei34 = -52.9383;
    fWei35 = -52.9938;
    fWei36 = -373.813;
    fWei37 = -274.226;
    fWei38 = 248.597;
    fWei39 = 87.6538;
    fWei40 = 206.085;
    fWei41 = -65.1376;
    fWei42 = -17.3287;
    fWei43 = -77.1919;
    fWei44 = 10.2998;
    fWei45 = 356.934;
    fWei46 = 31.2925;
    fWei47 = 127.591;
    fWei48 = 254.148;
    fWei49 = 108.609;
    fWei50 = 87.0099;
    fWei51 = 5.66207;
    fWei52 = -218.754;
```

```
fWei53 = 16.4265;
f0 = fI0;
f1 = 1.0;
f2 = 0.0;
f3 = 0.0;
f4 = 0.0;
f5 = 0.0;
f6 = 0.0;
f7 = 0.0;
f2 = f2 + f0 * fWei0;
f2 = f2 + f1 * fWei1;
f2 = f2 * 0.5;
f2 = (2.0 / (1.0 + exp(-2.0 * f2))- 1.0);
f3 = f3 + f0 * fWei2;
f3 = f3 + f1 * fWei3;
f3 = f3 * 0.5;
f3 = (2.0 / (1.0 + exp(-2.0 * f3))- 1.0);
f4 = f4 + f0 * fWei4;
f4 = f4 + f1 * fWei5;
f4 = f4 * 0.5;
f4 = (2.0 / (1.0 + exp(-2.0 * f4))- 1.0);
f5 = f5 + f0 * fWei6;
f5 = f5 + f1 * fWei7;
f5 = f5 * 0.5;
f5 = (2.0 / (1.0 + exp(-2.0 * f5))- 1.0);
f6 = f6 + f0 * fWei8;
f6 = f6 + f1 * fWei9;
f6 = f6 * 0.5;
f6 = (2.0 / (1.0 + exp(-2.0 * f6))- 1.0);
f7 = f7 + f0 * fWei10;
f7 = f7 + f1 * fWei11;
f7 = f7 * 0.5;
f7 = (2.0 / (1.0 + exp(-2.0 * f7))- 1.0);
f8 = 1.0;
f9 = 0.0;
f10 = 0.0;
f11 = 0.0;
f12 = 0.0;
f13 = 0.0;
f14 = 0.0;
f9 = f9 + f2 * fWei12;
f9 = f9 + f3 * fWei13;
f9 = f9 + f4 * fWei14;
f9 = f9 + f5 * fWei15;
f9 = f9 + f6 * fWei16;
f9 = f9 + f7 * fWei17;
f9 = f9 + f8 * fWei18;
f9 = f9 * 0.5;
f9 = (2.0 / (1.0 + exp(-2.0 * f9))- 1.0);
f10 = f10 + f2 * fWei19;
f10 = f10 + f3 * fWei20;
f10 = f10 + f4 * fWei21;
f10 = f10 + f5 * fWei22;
f10 = f10 + f6 * fWei23;
f10 = f10 + f7 * fWei24;
f10 = f10 + f8 * fWei25;
f10 = f10 * 0.5;
f10 = (2.0 / (1.0 + exp(-2.0 * f10))- 1.0);
f11 = f11 + f2 * fWei26;
f11 = f11 + f3 * fWei27;
f11 = f11 + f4 * fWei28;
f11 = f11 + f5 * fWei29;
f11 = f11 + f6 * fWei30;
f11 = f11 + f7 * fWei31;
f11 = f11 + f8 * fWei32;
f11 = f11 * 0.5;
f11 = (2.0 / (1.0 + exp(-2.0 * f11))- 1.0);
f12 = f12 + f2 * fWei33;
f12 = f12 + f3 * fWei34;
```

```
f12 = f12 + f4 * fWei35;
f12 = f12 + f5 * fWei36;
f12 = f12 + f6 * fWei37;
f12 = f12 + f7 * fWei38;
f12 = f12 + f8 * fWei39;
f12 = f12 * 0.5;
f12 = (2.0 / (1.0 + exp(-2.0 * f12))- 1.0);
f13 = f13 + f2 * fWei40;
f13 = f13 + f3 * fWei41;
f13 = f13 + f4 * fWei42;
f13 = f13 + f5 * fWei43;
f13 = f13 + f6 * fWei44;
f13 = f13 + f7 * fWei45;
f13 = f13 + f8 * fWei46;
f13 = f13 * 0.5;
f13 = (2.0 / (1.0 + exp(-2.0 * f13))- 1.0);
f14 = f14 + f2 * fWei47;
f14 = f14 + f3 * fWei48;
f14 = f14 + f4 * fWei49;
f14 = f14 + f5 * fWei50;
f14 = f14 + f6 * fWei51;
f14 = f14 + f7 * fWei52;
f14 = f14 + f8 * fWei53;
f14 = f14 * 0.5;
f14 = (2.0 / (1.0 + exp(-2.0 * f14))- 1.0);
fO0 = f9;
fO1 = f10;
fO2 = f11;
fO3 = f12;
fO4 = f13;
fO5 = f14;
fO0 = fO0 * (1 - (0 + 1 ) / 2.0) + (0 + 1) / 2.0;
fO1 = fO1 * (1 - (0 + 1 ) / 2.0) + (0 + 1) / 2.0;
fO2 = fO2 * (1 - (0 + 1 ) / 2.0) + (0 + 1) / 2.0;
fO3 = fO3 * (1 - (0 + 1 ) / 2.0) + (0 + 1) / 2.0;
fO4 = fO4 * (1 - (0 + 1 ) / 2.0) + (0 + 1) / 2.0;
fO5 = fO5 * (1 - (0 + 1 ) / 2.0) + (0 + 1) / 2.0;
```